Am J Nucl Med Mol Imaging 2020;10(6):349-374
www.ajnmmi.us /ISSN:2160-8407/ajnmmi0120161

Original Article

[^{68}Ga]Ga-PSMA-11 in prostate cancer: a comprehensive review

Frédéric Bois[1], Camille Noirot[1], Sébastien Dietemann[1], Ismini C Mainta[1], Thomas Zilli[2,3], Valentina Garibotto[1,3], Martin A Walter[1,3,4]

[1]Division of Nuclear Medicine, Diagnostic Department, University Hospital of Geneva, Geneva, Switzerland; [2]Division of Radiation Oncology, Oncology Department, University Hospital of Geneva, Geneva, Switzerland; [3]Faculty of Medicine, University of Geneva, Geneva, Switzerland; [4]Center for Biomedical Imaging (CIBM), Lausanne, Switzerland

Received August 12, 2020; Accepted November 15, 2020; Epub December 15, 2020; Published December 30, 2020

Abstract: Imaging of the prostate-specific membrane antigen (PSMA) has become an important tool for managing patients with recurrent prostate cancer, and one of the most frequently employed radiopharmaceuticals is [^{68}Ga]Ga-PSMA-11. Herein, we summarize the preclinical development and the clinical applications of [^{68}Ga]Ga-PSMA-11 and present side-by-side comparisons with other radiopharmaceuticals or imaging modalities, in order to assist imagers and clinicians in recommending, performing, and interpreting the results of [^{68}Ga]Ga-PSMA-11 PET scans in patients with prostate cancer.

Keywords: Prostate cancer, molecular imaging, staging, restaging, PSMA

Prostate cancer

Prostate cancer is one of the leading causes of morbidity and death in men in the Western world, and the second most common cancer in men worldwide. With an ever-aging population, the absolute number of men being diagnosed with prostate cancer is constantly increasing. In 2018, 1,276,106 new cases of prostate cancer were registered worldwide, representing 7.1% of all cancers in men [1]. In certain areas of the world, such as in the UK, more men die from prostate cancer each year than women die of breast cancer [2].

Screening tools for prostate cancer remain limited, primarily by means of prostate specific antigen (PSA) level assessment [3-5], treatment on the other hand has greatly improved in recent years [6]. The latest therapies approved include androgen receptor signaling with abiraterone acetate, enzalutamide and apalutamide, radiotherapy of bone metastases with radium-223 dichloride, immunotherapy with sipuleucel-T, and chemotherapy with taxane-based drugs. If current treatments are built on the synergistic effects obtained when using a combination of the aforementioned therapies, the next major leap forward is expected to stem from developments in the molecular characterization of stage-dependent markers.

Recurrence after primary therapy for prostate cancer occurs in 20 to 60% of cases [7, 8], and the 5-year survival rate in patients with high-volume metastatic disease is below 30% [9]. The historical mainstays of clinical examinations remain physical such as digital rectal examination, blood based in the form of PSA or tissue based in the form of trans-rectal or trans-perineal biopsies. However, these modalities present inherent diagnostic limitations.

Digital rectal examination has a positive predictive value between 5 and 30% in patients presenting low PSA values [10], it sometimes fails to identify clinically important prostate cancers, and it displays a high rate of high false positives [11]. Blood markers, such as PSA tend to be non-specific since they may be elevated by non-malignant clinical conditions such as prostatitis and benign prostatic hypertrophy. On the other

hand, low PSA does not necessarily rule out the presence of prostatic malignancy [12].

Conventional imaging techniques, such as Computed Tomography (CT) or multi-parametric magnetic resonance imaging (mpMRI), have been used to substantiate the diagnostic value. Given its poor sensitivity and specificity, anatomical diagnosis with CT of the prostate gland has been primarily used to stage the disease once diagnosis has been established. Computed tomography may reveal metastatic spread to pelvic lymph nodes, seminal vesicles, osseous metastases but is inherently based on changes in anatomy, particularly with regard to size. Thus, the failure to provide information pertaining to tumor metabolic activity limits its use to the early stage of disease. In the limited context for lymph node diagnosis, a recent analysis showed an acceptable specificity of 82% but unacceptable sensitivity of only 42% with CT [13].

The use of mpMRI has been increasing in frequency given its higher sensitivity, specificity and predictive value [14]. In addition to the detection of changes in architecture and anatomy of the prostatic gland, this imaging modality gives insights into the potential transformation of the tumor by assessing certain key parameters such as diffusion restriction and is also more accurate than CT in assessing the lymph nodes within the pelvis [15]. For all these reasons, mpMRI is gradually being implemented in the classical clinical workup of Prostate cancer [16].

Ultimately, diagnosis can only be affirmed by pathological assessment, usually with prostatic biopsy, but tissues may be obtained from biopsy material originating from prostatic metastatic foyers.

The prostate specific membrane antigen (PSMA)

In spite of the steady shift toward molecular imaging in clinical diagnostics, clinical imaging modalities for diagnosing cancer and monitoring treatment response have mostly remained at the anatomical rather than molecular level. For example, the historical Response Evaluation Criteria in Solid Tumors (RECIST) criteria [17], which are based on anatomical size, are still considered the reference standard in spite of its mere representation of what is happening at an anatomical size level. The overexpression of Prostate Specific Membrane Antigen (PSMA) in prostate cancer, which increases angiogenesis and increases metabolism of polyglutamated folates and uptake of monoglutamated folates, thus imparting a clear proliferative advantage [18], has been exploited as a molecular marker in the diagnostics of prostate cancer.

PSMA is a 750-amino acid trans-membrane protein found within the apical epithelium of secretory ducts of benign prostatic tissue. While its physiologic role in the prostate remains unclear, its enzymatic role in the cleavage of α-linked glutamate from N-acetylaspartyl glutamate and γ-linked glutamates from polyglutamated folates has been demonstrated [18]. The malignant transformation sees the translocation of PSMA to the luminal surface of the ducts [19] in addition to its overexpression, which is not found in other benign diseases such as prostatic hyperplasia [20].

Several other functions, such as involvement in cellular migration and nutrition, transport and signal transduction, have been attributed to PSMA [21]. Upon binding of a ligand, PSMA is internalized into the cell. In spite of its name, PSMA is not prostate specific as it can be found within lacrimal and salivary glands, the kidneys, liver, spleen and small intestine [22]. Its expression can be detected in tumor associated angiogenesis, glioblastoma, thyroid cancer, gastric, breast, renal and colorectal cancers [22].

PSMA boasts features, which can be exploited as a molecular target for imaging and therapy. Its high level of overexpression (100-1000 fold in 95% of prostate cancer cells) [22] and internalization upon binding [23], lead to enhanced specific uptake and retention, both vital factors for image quality and therapeutic efficacy. In addition, from a disease staging point of view, PSMA expression appears to correlate with advanced disease, castration resistant disease, Gleason score and PSA level [24, 25].

PSMA targeting agents

In spite of the typical issues related to antibody-based imaging agents, such as long circulation half-life, low signal to noise ratio and poor tar-

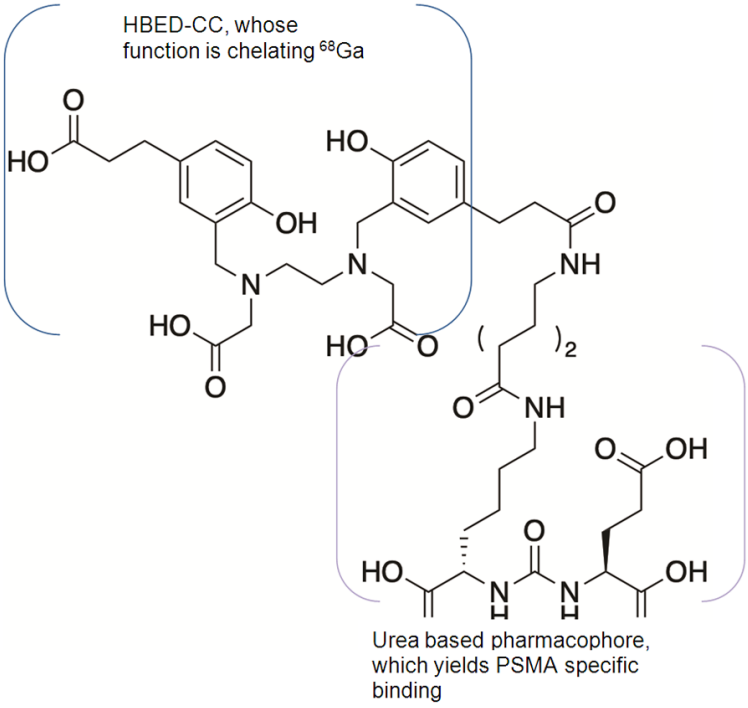

Figure 1. Structure of [68Ga]Ga-PSMA-11, with a representation of the two different substructures, HBED-CC for the chelation of [68Ga]Gallium and the urea-based pharmacophore for PSMA binding specificity.

get tissue uptake, two monoclonal antibodies (mAb) were developed targeting both the extracellular and intracellular epitopes of PSMA and demonstrated high affinity, specific and efficient targeting in vivo. The murine mAb 7E11 binds an intracellular domain of PSMA and the humanized mAb hJ591 binds to an extracellular domain of PSMA [26]. 7E11 was developed as a theranostic agent with parallel radiolabeling with ([111In]In ([111In]In-7E11, ProstaScint™) as a potential SPECT imaging agent [27, 28], and with [90Y]Y ([90Y]Y-7E11) as its therapeutic counterpart [29]. The high myelotoxic effect observed with [90Y]Y-7E11 ultimately stopped further development while the overall poor sensitivity with ProstaScint™ as a SPECT imaging agent gradually lead to its clinical demise. J591 mAb was clinically investigated for PET/CT imaging as [89Zr]Zr-hJ591 [30] and for therapy as [177Lu]Lu-hJ591 [31].

In parallel, small molecule PSMA-peptide inhibitors, devoid of inherent antibody specific limitations, have been successfully developed and are nowadays the mainstay of current PSMA imaging and therapy modalities [32]. A rational approach was used to develop these agents, with high PSMA affinity and rapid blood clearance as key parameters.

[68Ga]Ga-PSMA-11

Currently, [68Ga]Ga-PSMA-11 (Glu-NH-CO-Lys-(Ahx)-[[68Ga]Ga-HBED-CC] (HBED CC: N,N'-Bis(2-hydroxy-5-(ethylene-betacarboxy)benzyl)ethylenediamine N,N'-diacetic acid, **Figure 1**) is among the most widely used agents for prostate cancer PET/CT imaging. [68Ga]Ga-PSMA-11 belongs to the substance class of peptidomimetic PSMA inhibitors, a class of urea-based PSMA inhibitors first reported in 2001 [33]. Following its initial description and preclinical evaluation in 2012 [34], hasted development yielded the first clinical reports on [68Ga]Ga-PSMA-11 PET/CT imaging in 2012 and 2013 [35, 36].

[68Ga]Ga-PSMA-11 binding affinity

Upon radiolabeling, the size-demanding radiometal complexes often influence the affinity for the targeting molecule by changing the initial lipophilicity and/or charge. In particular in the case of small molecules, the pharmacological property can dramatically be reduced with respect to its binding properties. A study comparing linkers situated between the PSMA binding group 2-[3-(1,3-dicarboxypropyl)-ureido] pentanedioic acid (DUPA) and a 99mTc complex revealed that linker lipophilicity correlates positively with improved binding properties. A study further supported the idea that the PSMA active site is a pocket containing multiple potential interaction sites.

The pharmacophore was proposed to ideally present three carboxylic groups capable of interacting with the respective side chains of PSMA, one oxygen as part of zinc complexation in the active center and an aromatic structure able to interact with a hydrophobic part of the binding pocket [34, 37, 38]. These interactions were found to have positive additive effects on binding efficiency, which instigated the suc-

cessful development of the amphiphilic [68Ga]Ga-PSMA-11, a urea-based pharmacophore combined with a [68Ga]Ga-HBED-CC metal complex.

[68Ga]Ga-PSMA-11 was subsequently competitively analyzed for its binding capacity by performing an enzyme-based assay on rhPSMA (Naaladase-Assay) and a binding assay on LNCaP cells, an androgen-sensitive human prostate adenocarcinoma PSMA positive cell line [34]. The affinity related IC_{50} and calculated Ki values of both assays were found to be 7.5 ± 2.2 and 12.0 ± 2.8 nM respectively. For comparison purposes, in the same assay, IC_{50} and calculated Ki for the direct DOTA analog were found to be 19.4 ± 7.1 and 37.6 ± 14.3 nM respectively.

[68Ga]Ga-PSMA-11 uptake in LNCaP cells revealed that the HBED complex displays a significant increase in PSMA-specific internalization when compared with its DOTA analog. In a cell uptake experiment, three different concentrations of HBED and DOTA radiolabeled compounds were given to either LNCaP or PC-3 cells, a PSMA negative cell line derived from bone metastasis of grade IV of prostate cancer. Specific uptake in LNCaP was substantially higher for [68Ga]Ga-PSMA-11, while unspecific uptake in PC-3 cells was significantly lower when compared to the DOTA analog. Thus, despite nearly identical binding affinity, the presence of HBED and DOTA complexes induce clear differences in specific and unspecific cell uptake.

Influence of diastereoisomers of HBED-CC on [68Ga]Ga-PSMA-11 binding

As previously mentioned, the structure of the active site of a PSMA inhibitor consists of two independent main binding sites, a zinc-containing rigid site and a rather lipophilic efferent tunnel [38]. The urea-based portion of PSMA inhibitors typically interacts with the carboxylic groups and the carbonylic oxygen. However, efficient internalization of a PSMA-directed radiotracer requires the interaction of the linker region of the molecule with hydrophobic tunnel region. Due to the specific nature of the interaction, slight chemical differences caused by the known formation of the three different diastereoisomers of HBED-CC after gallium-complexation might influence the binding properties of the whole molecule.

High thermodynamic stability constants are observed for the complexation of gallium with HBED ($>10^{39}$), which structure is acyclic and requires low energy for complex formation. As a consequence, labeling is fast even at ambient temperature and yields a complex with high kinetic stability at physiological pH [39], in vivo [40] and in human serum for at least 72 hours [41]. These features render HBED extremely attractive as a gallium chelator for high-stability labeling of radiopharmaceuticals. However, in contrast to other clinically radiometal cyclic chelators, HBED-CC can form three NMR-identifiable diastereoisomers (namely RR, RS and SS) during gallium complexation, with RR thermodynamically favored [40]. In spite of the fact that experimental in vitro studies have shown that the two main species observed (RR and RS) have identical binding properties toward PSMA (IC50 values: 24.8 ± 1.2 nM and 27.4 ± 1.3 nM respectively) [38], the presence of two different radioisomers in a variable ratio form batch to batch is unacceptable from a quality control perspective in a clinical setting.

For this reason, in a standard GMP-compliant synthesis labeling protocol, [68Ga]Ga-PSMA-HBED-CC is incubated at 85°C to favor the formation of the thermodynamically more stable diastereoisomer RR, but RS is still present in small amount in the labeling reaction mixture even at high labeling temperature. Its presence, however, does not have any significant negative influence on the PSMA-binding properties and therefore on image quality.

[68Ga]Ga-PSMA-11 in vivo biodistribution

One hour following tail vein injection of 1-2 MBq [68Ga]Ga-PSMA-11 in mice (0.1-0.2 nmol) the animals were sacrificed and their organs of interest were dissected, blotted dry, and weighed. The radioactivity was measured with a gamma counter and calculated as % ID/g [34]. [68Ga]Ga-PSMA-11 was cleared rapidly from the blood and PSMA negative tissue. Liver activity represented a mere 0.87 ± 0.05% ID/g as early as one hour after injection. Accumulation in kidney, spleen, and lung uptake was high with 139.4 ± 21.4% ID/g, 17.90 ± 2.87% ID/g, and 2.49 ± 0.27% ID/g respectively, and could be completely blocked to 4.02 ± 1.14%

ID/g, 1.54 ± 0.33% ID/g, and 0.64 ± 0.32% ID/g respectively following the co-injection of 2 mg/kg 2-(phosphonomethyl)pentanedioic acid (PMPA), a PSMA inhibitor. Tumor uptake amounted to 7.70 ± 1.45% ID/g on LNCaP and 1.30 ± 0.12% ID/g on PC-3.

To substantiate the claim that reduced kidney accumulation of [68Ga]Ga-PSMA-11 after PMPA co-administration is PSMA specific, a side-by side comparison of both D- and L-forms of [68Ga]Ga-PSMA-11 was initiated. PET dynamic time−activity curves revealed that the D-form is cleared rapidly from the kidney while [68Ga]Ga-PSMA-11 is accumulating with little bladder excretion. This result is most likely linked to the 103-fold difference in PSMA affinity of D-[68Ga]Ga-PSMA-11 [34].

[68Ga]Ga-PSMA-11 in vivo imaging

MicroPET studies were conducted by injection of 10-25 MBq of [68Ga]Ga-PSMA-11 via a lateral tail vein into mice bearing LNCaP tumor xenografts [34]. The anesthetized animals were placed into a small animal PET scanner and 50 min dynamic microPET scans, starting at 1 min post injection followed by a 20 min static scan, were recorded. The organ and tumor uptake value of the [68Ga]Ga-PSMA-11 was reflective of in vitro data since [68Ga]Ga-PSMA-11 cleared rapidly from the blood and PSMA negative tissues.

Liver activity was limited to only 0.87 ± 0.05% ID/g as early as one hour following injection. Uptake was found to be high in kidney (139.4 ± 21.4% ID/g), spleen (17.90 ± 2.87% ID/g) and lung (2.49 ± 0.27% ID/g). These uptakes were nearly completely blocked down to 4.02 ± 1.14% ID/g, 1.54 ± 0.33% ID/g, and 0.64 ± 0.32% ID/g, respectively, after the co-injection of 2 mg/kg of PMPA. Tumor uptake amounted to 7.70 ± 1.45% ID/g on the PSMA positive LNCaP and 1.30 ± 0.12% ID/g on PSMA negative PC-3 cell lines.

Using a model of monoclonal cell lines, where PSMA expression was differential, but tumor sizes comparable at around 5 mm of diameter, the relationship between absolute surface PSMA target expression of biopsy samples of prostate cancer, and imaging signal with [68Ga]Ga-PSMA-11 was assessed in a murine model [42]. The use of PROMISE criteria guided the visual interpretation based on reference organ uptake [43] of [68Ga]Ga-PSMA-11.

PET/CT scans were then performed on days 7 and 8, and PSMA expression was quantified on days 7 and 8 by flow cytometry of fine needle aspiration tumor biopsies. In this model, where cell surface PSMA expression was correlated with PET signal, and about 20,000 PSMA molecules per tumor cell surface were identified as threshold for positive PET reading. This threshold is about 10-times lower than the known surface expression in typical human prostate cancer cell lines LNCaP and C4-2 (~190,000 and 240,000 receptors per cell, respectively).

These findings suggest that the threshold for preclinical PET positivity is quite low. On the other hand, while PSMA PET imaging seems to be able to detect small changes in PSMA molecules/cell at a low expression level, this sensitivity disappears at higher PSMA levels, with a mere 1.2-fold PET signal increase for an increase of 22,000 to 45,000 PSMA/cell. Limitations to the accuracy of quantitative PET imaging and the direct value of this side-by-side comparison depends on scanner-specific factors, such as spatial resolution, sensitivity; the characteristics of the radiopharmaceutical, e.g. specific activity (the ratio of radiolabeled and "cold" masses) as well as biological variables, e.g. receptor saturation.

[68Ga]Ga-PSMA-11 toxicity

In the absence of regulatory guidelines, the mass amount of [68Ga]Ga-PSMA-11 allowed to be injected in humans was, for the longest time, a subject of personal appreciation. However, a circulated draft of a European monography for [68Ga]Ga-PSMA-11, indicates a maximum amount of 30 microg per injection.

[68Ga]Ga-PSMA-11 dosimetry in humans

The effective dose and organ doses from injection of [68Ga]Ga-PSMA-11 in a cohort of low-risk prostate cancer patients [44] was recently reported from an injection with 133-178 MBq of [68Ga]Ga-PSMA-11 in a cohort of six patients, followed by PET/CT acquisitions, urine and venous blood collection up to 4h post injection. In this study, [68Ga]Ga-PSMA-111 was rapidly cleared from the blood and accumulated preferentially in the kidneys and the liver, and the

Table 1. Physiological uptake of [68Ga]Ga-PSMA-11 (adapted from [47])

		Median SUV_{max}	SUV_{max} Range
Lachrymal gland		7.5	3.0-25.9
Nasal mucosal lining		4.0	1.7-8.8
Parotid gland		16.1	5.5-30.9
Sub-mandibular gland		17.3	7.5-30.4
Liver		6.8	2.8-13.0
Spleen		9.1	3.8-36.7
Kidney		49.6	2.7-97.0
Duodenum		13.8	5.8-26.9
Pancreas	Head	2.9	1.1-7.6
	Body	2.7	1.2-8.6
	Tail	3.3	1.6-8.1
Colon		1.6	0.5-2.7
Blood pool (aorta)		1.8	0.8-3.2
Adrenal glands		1.8	0.6-3.4
Bone marrow (over the iliac bone)		0.7	0.2-1.8
Lymph nodes with fatty hilum		1.8	1.5-2.2
Prostate gland		2.2	1.7-2.9

associated effective dose was 0.022 mSv/MBq. Kidneys and lacrimal glands receiving the highest organ dose, with 40 mGy and 0.12 mGy per MBq administered respectively.

Current joint Society of Nuclear Medicine and Molecular Imaging (SNMMI) and European Association of Nuclear Medicine (EANM) guidelines recommend a dose of 1.8-2.2 MBq (0.049-0.060 mCi) per kilogram (kg) body weight (BW) [45]. A recent attempt to assess image quality with decreased dose revealed a substantial negative impact on image quality and lesion detectability [46].

[68Ga]Ga-PSMA-11 biodistribution in humans

The distribution of [68Ga]Ga-PSMA-11 is linked to the epithelial expression of the target protein PSMA present in the various tissues and to the physiological excretion of the radiopharmaceutical [47]. Therefore, physiological [68Ga]Ga-PSMA-11 uptake is mainly observed in the urinary bladder, the kidneys and the ureters, due to urinary excretion. It is also observed in parotid and submandibular glands due to salivary excretion, in lachrymal glands, and in the colon due to digestive excretion. Finally, it is found in the reticulo-endothelial system, e.g. the spleen and the liver, in the prostate gland, the pancreas, the adrenal glands, and autonomic ganglia. Indicative values of intensity of the activity (SUV_{max}) of the different tissues and background are summarized in **Table 1** (adapted from [47]).

False positive findings with [68Ga]Ga-PSMA-11

The comprehensive pathophysiological mechanism of [68Ga]Ga-PSMA-11 uptake is not defined for all tissues. Thus, in addition to the physiological distribution and specific uptake in prostate tumor tissues, also specific uptake in other tissues is known. This uptake can interfere with the image analysis, both in malignant and benign lesions. Therefore, as part of the image interpretation, radiopharmaceutical uptake intensity should be taken in consideration, since signal to background ratio is positively correlated with diagnostic accuracy, for the localization of radiopharmaceutical uptake, with regards to typical tumor drainage territory and for presence of underlying morphological abnormalities.

Clinical use of PET with [68Ga]Ga-PSMA-11 and other PSMA radiopharmaceuticals, revealed consistent and significant uptake in minor and major salivary glands [48]. This uptake is still not well understood, but could lie in the biology of the glands themselves, given the prevalence of secretory granules that potentiate formation of radiation-induced free radicals present in this type of tissue. With the steady increase in PSMA radioligand therapies, it is of vital importance to understand the underlying reasons since therapeutic radiations severely damage these glands. External cooling of the salivary glands was initially performed in the clinic with the expectation to reduce uptake due to vasoconstriction. However, the technique ultimately failed to prove relevant in a systematic analysis and probably finds its explanation in the form of local hyper-perfusion to restore the crucial blood supply to the organs near the head [49]. So far, the only autoradiography and immunohistochemistry study [50], focused on the accumulation of PSMA-targeting radioligands in samples of submandibular gland human tissues, recently provided evidence that this accumulation in submandibular gland is not primarily a result of PSMA-mediated uptake.

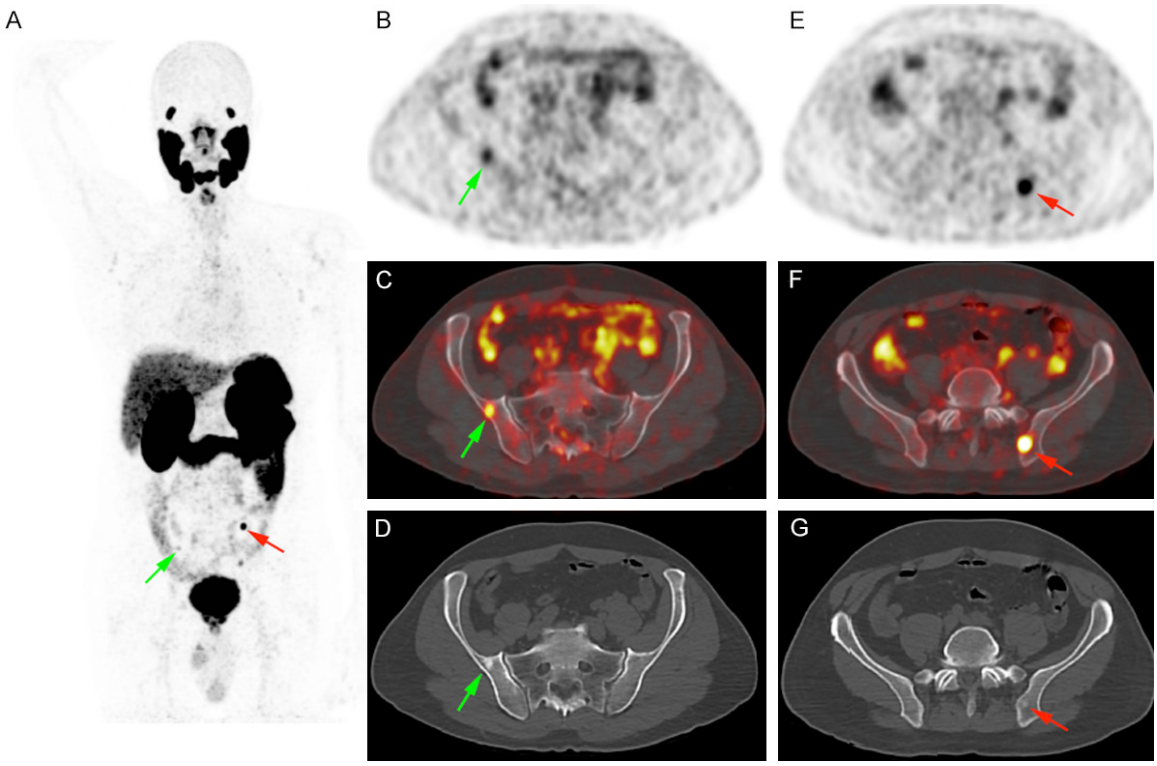

Figure 2. Prostate cancer staging in a 54 years old patient (Gleason score 4 + 4, PSA value: 8.6 ng/ml) showing two blastic lesions with focal [^{68}Ga]Ga-PSMA-11 uptake (maximum Standardized Uptake Value measured at 13). The patient underwent surgery and PSA was undetectable after surgery, proving the non-specific nature of these lesions.

False positives are related to benign lesions that can mimic distant metastases or lymphatic dissemination. In vitro immune-histochemical expression of PSMA by the autonomous system was confirmed when [^{68}Ga]Ga-PSMA-11 increased uptake was shown in ganglia of the autonomic nervous system [51]. Frequently reported locations include celiac ganglia [51] and the sympathetic chains at the cervical, thoracic and sacral level [51-53]. Uptake at the celiac level can be mistaken for retroperitoneal metastases of prostate cancer, and is therefore more challenging to properly diagnose than isolated uptake which, without other pathological foci of uptake in the retroperitoneal or pelvic region, is more likely to be of benign origin [51, 52].

Granulomatous inflammatory diseases such as Wegener's disease [47] and sarcoidosis, with typical mediastino-hilar ganglionic involvement [54-57], can show increased [^{68}Ga]Ga-PSMA-11 uptake. Yet, in the latter, bilateral and symmetrical distribution of the radiotracer within mediastino-hilar lymph nodes is expected. In addition, selective endothelial expression of PSMA receptor may result in tracer uptake in pleura and heart valves [58, 59].

Secondary bone dissemination of prostatic adenocarcinoma is relatively common. As such, benign bone lesions showing increased [^{68}Ga]Ga-PSMA-11 uptake might represent a diagnostic challenge, as reported for osseous hemangioma [60-62], fibrous dysplasia [63], Paget's disease [64-70] and fractures [71, 72]. The uptake observed in osseous and extraosseous hemangioma is thought to be related to increased lesion vascularization and endothelial cells number. An example of false positive focal bone uptake is shown in **Figure 2**.

Systemic diseases might also mimic visceral metastases, such as tuberculosis [73] and sarcoidosis, e.g. in the lungs or the liver [56, 57]. Nervous system lesions such as meningioma [74, 75], schwannoma [76, 77], peripheral nerve sheath tumor [78], and cerebral infarction [79, 80] have also been reported to exhibit increased uptake. Finally, soft tissue lesions

Table 2. Non-prostatic benign PSMA-avid lesions (adapted from [104])

Diagnostic	Reference(s)
Sarcoidosis	[54-57]
Reactivated tuberculosis	[73]
Benign lung opacities and bronchiectases	[174]
Anthracosis	[175]
Paget's disease	[64-70]
Vertebral body fracture	[72]
Healing sacral fracture	[71]
Benign fibrous dysplasia	[63]
Schwannoma	[76, 77]
Meningioma	[74, 75]
Peripheral nerve sheath tumor	[78]
Hemangioma	[60-62]
Intramuscular myxoma	[83]
Acrochordon	[85]
Dermatofibroma	[86]
Pseudo-angiomatous stromal hyperplasia of breast	[82]
Desmoid tumor	[84]
Fasciitis nodularis	[81]
Pancreatic serous cystadenoma	[176]
Follicular thyroid adenoma	[177, 178]
Lipid-rich adrenal adenoma	[179]
Herniated spleen	[180]
Senile seminal vesicle amyloidosis	[181]
Cerebral infarction	[79, 80]

can wrongfully be diagnosed as metastatic sites for prostatic adenocarcinoma since focal uptake has been reported for fascitis nodularis [81], pseudo-angiomatous stromal hyperplasia [82], intramuscular myxoma [83], desmoid tumor [84], acrochordon [85] and dermatofibroma [86].

A summary of the published reports on detection of non-prostatic benign PSMA-avid lesions in the staging/restaging work-up of prostate cancer, i.e. false-positive findings, is provided in **Table 2**.

False negative findings with [68Ga]Ga-PSMA-11

Prostate cancer lesions lacking increased PSMA expression, leading to false negative findings, have been reported, and can be associated with primary histology and metastatic localization. Immunohistochemistry studies have shown that PSMA-negative primary prostate cancer have a rare occurrence of less than 3% [25, 87] and can be correlated with the uptake of [68Ga]Ga-PSMA-11 in primary prostate cancers [88]. In addition, neuroendocrine differentiation has been associated with negative PSMA-based imaging [89-91]. Immunohistochemistry also showed that PSMA expression is highest in primary cancer lesions in 88 to 100% of nodal metastases [92], while bone metastases can be negative in up to 15% of cases [25].

[68Ga]Ga-PSMA-11 uptake in other malignant lesions

The main reason for specific [68Ga]Ga-PSMA-11 uptake in non-prostatic malignancies is the epithelial expression of PSMA linked to neo-vascularization [93, 94]. Several types of cancer have already been reported to display [68Ga]Ga-PSMA-11 uptake. The histology most commonly reported for its elevated PSMA expression, confirmed by immunohistochemical studies, is renal cell carcinoma [95-102], particularly clear cell renal cell carcinoma, followed by chromophobe renal cell carcinoma [98, 103]. A summary of the reported incidental detection of non-prostatic malignant PSMA-avid lesions in the staging/restaging work-up of prostate cancer is provided in **Table 3** (adapted from [104]).

[68Ga]Ga-PSMA-11 for restaging of prostate cancer

Since measuring sensitivity and specificity for patients with recurrent prostate cancer is limited by the lack of a reference standard, studies often use detection rate as outcome in evaluation the usefulness of [68Ga]Ga-PSMA-11 in prostate cancer restaging, considering by definition positive all patients in biochemical recurrence, namely with a PSA above 0.2 ng/mL [105].

The detection rate of [68Ga]Ga-PSMA-11 in recurrent prostate cancer has been extensively investigated. Findings from the two largest meta-analyses and a large prospective study

Table 3. Non-prostatic malignant PSMA-avid lesions (adapted from [104])

Diagnosis	References
Follicular lymphoma	[182, 183]
Follicular thyroid carcinoma	[184]
Papillary thyroid carcinoma	[97], [185]
Hurthle cell adenoma	[185]
Multiple myeloma	[186]
Gastrointestinal stromal tumor	[187]
Pancreatic neuroendocrine tumor	[188]
Hepatocellular carcinoma	[189, 190]
Rectal adenocarcinoma	[191, 192]
Squamous cell carcinoma of the oropharynx	[193]
Primary lung cancer	[73], [194]
Penile squamous cell carcinoma	[195]
Colon adenocarcinoma	[196]
Urothelial carcinoma of ureter	[197]
Renal cell carcinoma	[97, 198, 199]

are that the detection rate ranges from 74 to 81%, and that the pooled estimated rate of positive scans are correlated with the PSA level [106-109]. Specifically, the rate of positive scans was 42-57% for PSMA levels of 0.2-0.99 ng/mL, 58-84% for PSMA levels of 1.0-1.99 ng/mL, 76% for PSMA levels of 2.0-2.99 ng/mL, and 95% for PSMA levels above 2 ng/mL.

Sensitivity and specificity in the context of recurrent prostate cancer has been measured only in limited patient cohorts using histopathology as gold standard. Here, salvage lymphadenectomy after [68Ga]Ga-PSMA-11 imaging of 308 lesions in 28 patients was correlated with 87% per-lesion sensitivity and 93% specificity [110]. [68Ga]Ga-PSMA-11 diagnostic performance estimates, using a lymphatic main region-based approach and a subregion-based approach, were derived from for 965 resected lymph nodes in 30 patients [111]. Sensitivity, specificity, negative predictive value, positive predictive value, and accuracy for the main region-based approach were 92%, 100, 100%, 89%, and 96, and for the subregion-based approach 81%, 100%, 99%, 93%, and 94%.

The clinical nomogram, proposed to predict [68Ga]Ga-PSMA-11PET/CT positivity in different clinical settings of PSA failure proved good accuracy in predicting a positive scan with values ≥ 40% [112], providing the most informative cutoff in counseling patients to [68Ga]Ga-PSMA-11 PET/CT and could be used as an important tool to guide to clinicians in the best use of PSMA-based PET imaging.

In an effort to assess the frequency of [68Ga]Ga-PSMA-11 positive lesions outside the standard salvage radiotherapy planning volumes using the Radiation Therapy Oncology Group (RTOG) guidelines, 270 subjects with recurrent prostate cancer after radical prostatectomy and PSA levels < 1 ng/mL were investigated [113]. Fifty-two patients (19%) had at least one [68Ga]Ga-PSMA-11-positive lesion not covered by the consensus target volumes, consisting mainly of bone lesions (in 23/52) and perirectal lymph nodes (16/52).

On the other hand, in order to evaluate the impact of [68Ga]Ga-PSMA-11 imaging on TNM stage and radiotherapy planning as compared with conventional imaging using bone scan and/or CT or MRI, two cohorts consisting of 11 patients with persistent PSA after radical prostatectomy and 60 with PSA increase after primary treatment were studied [114]. The latter consisted of 23 subjects after RP, 5 after RT and 32 after radical prostatectomy followed by salvage radiotherapy. Respective mean PSA levels were 1.27 ng/mL and 1.1 ng/mL for the two groups. The identification of additional lesions with [68Ga]Ga-PSMA-11 scans resulted in a change in TNM stage in 51% and change in radiotherapy plan in 56% of cases. An example of nodal metastasis in a case of biochemical recurrence only detected by [68Ga]Ga-PSMA-11 PET imaging is shown in **Figure 3**.

A retrospective review of patients scanned with [68Ga]Ga-PSMA-11 for biochemical recurrence following radical prostatectomy with PSA ≤ 2.0 ng/mL was performed to assess if the recurrent disease was within standard radiation target volumes [115]. Through a comparison of patients and clinical variables between men with recurrences covered by standard salvage radiation fields and those with recurrences outside of standard fields, PSMA-avid disease was observed in 53% of patients. For these patients, 38% had PSMA-avid recurrence found outside of the pelvis, 50% lesions confined to the pelvic lymph nodes and prostatic bed, and 12% in the prostate bed only. In addition, salvage radiation including standard Intensity Modulated Radiation Therapy (IMRT) pelvic nodal volumes did not cover PSMA-avid nodal

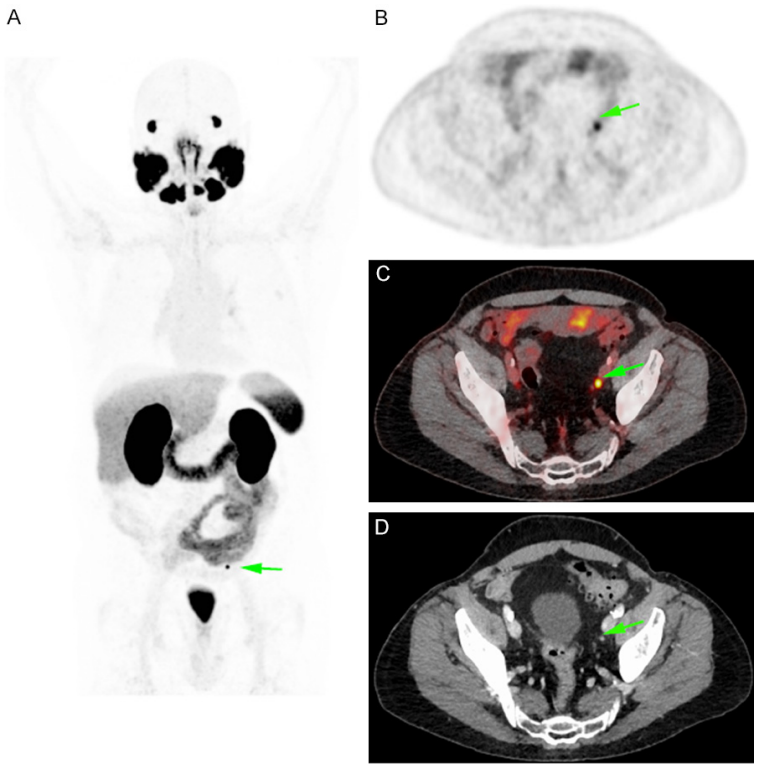

Figure 3. Restaging in a 74 years old patient in biochemical recurrence (PSA value: 0.2 ng/ml) showing only one lymph node measuring 4 mm and with a focal [68Ga]Ga-PSMA-11 uptake (maximum Standardized Uptake Value measured at 15).

disease in 30% of patients. Therefore, routine use of PSMA-PET imaging in the early salvage setting may potentially lead to treatment optimization by improving target coverage, by using dose escalation to the local or nodal relapse [116-118] or by performing metastasis-directed therapies for oligometastatic patients [119].

A meta-analysis including over a thousand patients showed an overall change in management in 54% of cases (95% CI: 47-60%) following [68Ga]Ga-PSMA-11 imaging [120]. In particular, in the population of patients with recurrent prostate cancer, there was an increase in the proportion of patients treated with curative approaches including radiotherapy, surgery, focal therapy and multimodal treatment, and reduction of patients treated solely with systemic medications or untreated.

Ongoing prospective phase III trials randomizing between standard salvage radiotherapy with or without a restaging PSMA PET/CT [121] will certainly help to determine in the near future if molecular imaging can improve outcome in patients with early biochemical relapse after radiotherapy.

[68Ga]Ga-PSMA-11 for initial staging of prostate cancer

The excellent diagnostic performance of [68Ga]Ga-PSMA-11 in restaging motivated its investigation also in the initial staging of the disease, namely in patients at high risk for metastatic disease. Multiple studies suggested high diagnostic accuracy also in this indication [122-124]. An example of metastatic nodal and bone spread at staging detected by [68Ga]Ga-PSMA-11 is shown in **Figure 4**. This was recently confirmed by a prospective randomized multicenter study assessing the impact of [68Ga]Ga-PSMA-11 PET for initial staging of high-risk prostate cancer prior to curative treatment, compared with conventional imaging by CT and bone scanning. On the basis of these findings, PSMA PET/CT should be the imaging modality of choice in the primary staging of high-risk prostate carcinoma, given the superior accuracy as compared with conventional imaging, combined with lower overall radiation exposure and higher reporter agreement. PSMA imaging can also be used to guide radiotherapy treatment of oligometastatic de novo prostate cancer [119], the next investigational step in the management of low burden synchronous disease after the evidence of an overall survival benefit of a local radiotherapy [125]. Of note, ongoing clinical trial such as the EORTC 1414 PEGASUS trail (ClinicalTrials.gov Identifier: NCT02799706) already implement modern imaging techniques in the curative treatment of de novo oligometastatic prostate cancer patients.

[68Ga]Ga-PSMA-11 versus other radiopharmaceuticals and imaging modalities

[68Ga]Ga-PSMA-11 vs. [18F]F-, [18F]F-Methyl-, [18F]F-Ethyl- or [11C]-choline

[68Ga]Ga-PSMA-11 was first used in humans in 2011 [35], and shortly thereafter became the new PET imaging reference standard for prostate cancer, as it clearly outshone [18F]F-choline,

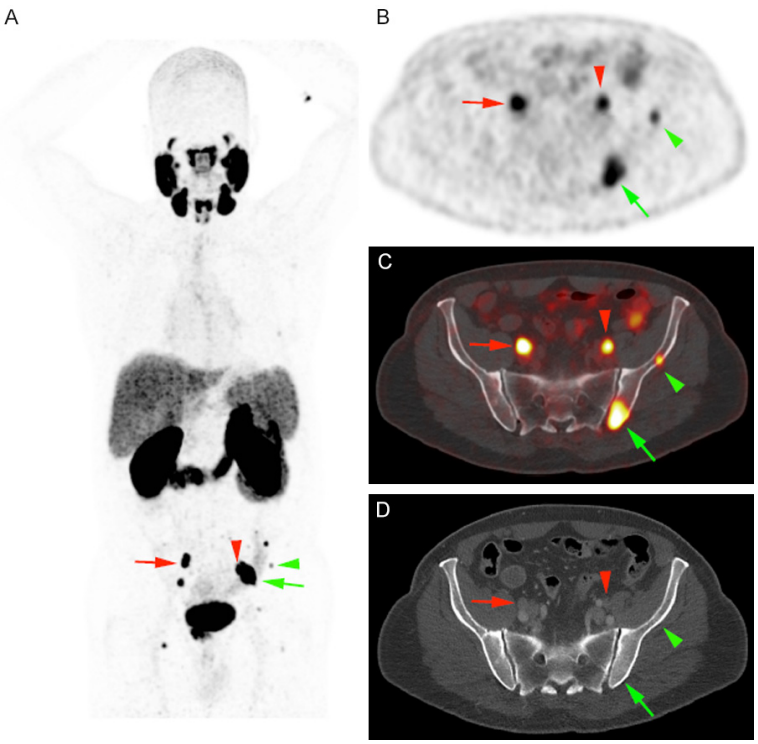

Figure 4. Prostate cancer staging in a 68 years old patient (Gleason score 4 + 3, PSA value: 13.5 ng/ml) showing local disease associated with multiple nodal (red arrows) and bone (green arrows) metastatic lesions. PET imaging induced a change in management towards docetaxel and androgen deprivation.

Table 4. Detection rate of [68Ga]Ga-PSMA-11 vs. [18F]F-choline in prostate cancer

PSA level (ng/mL)	[68Ga]Ga-PSMA-11 vs. [18F]F-choline (%)		
	Ref [126]	Ref [126]	Ref [127]
<0.5		50/12	
<1			61/46
<2		71/36	
1-2			81/66
<2.82	69/44		
>2.82	100/90		
>2		88/63	97/89
>5			

the primary clinical diagnostic PET radiopharmaceutical of the time, or some of its analogs such as [18F]F-Methylcholine, [18F]F-Ethylcholine or [11C]choline. A clear superiority was demonstrated in various aspects of side-by-side comparisons.

Parallel injections of [68Ga]Ga-PSMA-11 and [18F]F-choline, [18F]F-Methylcholine, [18F]F-Ethylcholine or [11C]choline were performed to assess their respective lesion detection performance in several studies. Overall significant superior diagnostic performance of [68Ga]Ga-PSMA-11 was consensual [110, 126-129]. [68Ga]Ga-PSMA-11 also allowed systematical identification of more lesions at lower PSA values than [18F]F-choline [126, 127], as summarized in **Table 4**.

In a prospective study of prostate cancer patients with biochemical relapse, histology of all lesions indicated by imaging was performed [110]. Patients underwent [18F]F-Ethylcholine and [68Ga]Ga-PSMA-11 PET scans. All patients with positive lymph nodes on imaging were submitted to pelvic and/or retroperitoneal lymphadenectomy. Per-lesion analysis showed an accuracy of 92% (95% CI, 88%-95%) for [68Ga]Ga-PSMA-11 versus 82% (95% CI, 88%-95%) for [18F]F-Ethylcholine. The negative predictive value (NPV) was 97% (95% CI, 93%-98%) for [68Ga]Ga-PSMA-11 versus 88% (95% CI, 84%-92%) for [18F]F-Ethylcholine. There was a clear trend towards higher sensitivity, specificity and negative predictive value. Per-patient, there was a positive predictive value of 82% for [68Ga]Ga-PSMA-11 and 79% for [18F]F-Ethylcholine.

Side-by-side comparison of uptake of [68Ga]Ga-PSMA-11 with [18F]F-choline showed a higher value for [68Ga]Ga-PSMA-11 in 79% of lesions, lower in 15% and equal in 5% of all cases [126]. Tumor-to-background ratio was clearly superior in 95% of lesions with [68Ga]Ga-PSMA-11 as increased uptake observed with [18F]F-choline, can be hampered by relatively high background activity. The most significant differences observed between the two radiopharmaceuticals regarding tumor uptake, and even more when it comes to tumor-to-background ratio, were observed in lymph node metastases followed by the bone lesions, local recurrences and soft tissue metastases.

Patient management after [68Ga]Ga-PSMA-11 and [18F]F-Methylcholine imaging [128] was impacted in 63% of cases overall, 54% based on [68Ga]Ga-PSMA-11 results alone and 29% on [68Ga]Ga-PSMA-11 and [18F]F-Methylcholine as equals. Patients with early biochemical relapse after radical prostatectomy are usually treated with salvage radiotherapy of the prostatic bed even in the absence of imaging findings. However, in the patient cohort of this study, 75% of the [68Ga]Ga-PSMA-11 positive patients with low PSA had disease outside the prostatic bed.

Among a pool of bone lesions detected by imaging from a cohort of 103 patients, a per-lesion-analysis showed that 62% were identified by both [68Ga]Ga-PSMA-11 and [11C]choline, 36% were visible with [68Ga]Ga-PSMA-11 solely and 2% with [11C]choline alone [129]. Overall, the 98% detection rate observed with [68Ga]Ga-PSMA-11 was significantly higher as the 64% detection rate of [11C]choline. The per-patient-analysis revealed that 31% of lesions were detected by both radiopharmaceuticals, 3% by [68Ga]Ga-PSMA-11 alone, and 1% by [11C]choline alone.

For distant metastases, [68Ga]Ga-PSMA-11 and [11C]choline seem to have complementary roles. [68Ga]Ga-PSMA-11 detected significantly more patients with N1 stage in a cohort of patients with local lymph node metastases detected by imaging [129]. Thereby, 70% were classified N1 by both radiopharmaceuticals, 25% additional patients were upstaged to N1 after [68Ga]Ga-PSMA-11 imaging, and 1.5% were positive with [11C]choline alone. For distant metastases, staging was in agreement with both radiopharmaceuticals in 77% and discordant in 11% of all cases. Patients were upstaged after [68Ga]Ga-PSMA-11 PET scan in 6% of all cases as compared to 5% on [11C]choline results alone.

Regarding oligometastatic disease, a significant difference between the results with [68Ga]Ga-PSMA-11 and [11C]choline was observed since 16% considered oligometastatic with [11C]choline alone were found to have more than 3 metastases with [68Ga]Ga-PSMA-11. On the other hand, 4% of patients deemed oligometastatic with [68Ga]Ga-PSMA-11 were found to be multi-metastatic with [11C]choline. Overall, 45% of the oligometastatic patients were identified with both radiopharmaceuticals, while 35% were found to have more than 3 lesions by both compounds.

Regarding initial staging, significantly more suspicious lymph nodes and bone lesions were detected by [68Ga]Ga-PSMA-11 compared to [11C]choline in the lesion-based analysis ($P< 0.004$), but without a significant difference in the patient-based analysis ($P=0.625$).

[68Ga]Ga-PSMA-11 vs. [18F]F-DCFPYL

[68Ga]Ga-labelled PSMA-radiopharmaceuticals have been systematically phased out by fluorine-18-labeled analogs given the advantages provided by [18F]Fluoride as compared to [68Ga]Gallium: key features are the longer half-life (109 min vs. 68 min), the cyclotron produced large centralized batches (vs. generator-produced [68Ga]Gallium), and the lower positron energy in favor of spatial resolution and reduced blurring effects.

Introduced in 2015, [18F]F-DCFPYL is a front runner [18F]F-labeled candidate for targeting PSMA with PET in the clinic. Systematic head-to-head comparison of the number of lesion positive results obtained, as compared to [68Ga]Ga-PSMA-11, in 14 prostate cancer in biochemical relapse was performed [130]. Outcome measures, such as number of detected PSMA-positive lesions, tumor uptake value (SUV_{max}) and lesion to background ratio were assessed. All suspicious lesions identified by [68Ga]Ga-PSMA-11 were also detected with [18F]F-DCFPYL while in three patients, the latter allowed identifying additional lesions. [18F]F-DCFPYL also significantly outperformed [68Ga]Ga-PSMA-11 in the mean SUV_{max} measures (14.5 vs. 12.2, $P=0.028$), as well as mean tumor to background ratio. However, the differences in SUV_{max} were only found to be significant with the use of kidney, spleen, or parotid as reference organs ($P=0.006$, $P=0.002$, $P=0.008$), but not using the liver ($P=0.167$) or the mediastinum ($P=0.363$).

[68Ga]Ga-PSMA-11 vs. [18F]F-fluciclovine

Since 2016, [18F]F-fluciclovine (Axumin®, Blue Earth Diagnostics Ltd.) is the only PET imaging agent approved by the FDA in the US in the limited context of localization of recurrent prostate

cancer. It is deemed "usually appropriate" by the American College of Radiology Appropriateness Criteria in the post-prostatectomic follow-up of prostate cancer patients, and after nonsurgical pelvic and local treatment in case of concern for recurrence.

Head-to-head comparison studies are still limited [131-133] and the relative values of each imaging modality were debated [134, 135]. [68Ga]Ga-PSMA-11 demonstrated overall higher rates detection but with high variability between cohorts and depending of sites of recurrent cancer. The key advantage of [18F]F-fluciclovine lies in its capacity to detect localized foyers in close anatomical relation to the urinary bladder, an area where the accumulation of [68Ga]Ga-PSMA-11 hinders the detection. On the other hand, [68Ga]Ga-PSMA-11 alone was able to detect recurrences in bone, other organs and extra-pelvic lymph node sites.

[68Ga]Ga-PSMA-11 vs. [18F]F-PSMA-1007

[18F]F-PSMA-1007, another [18F]F-PSMA targeting agent has been recently introduced in the clinic. In addition to the aforementioned advantages provided by fluorine-18-fluoride, its key advantages lie in its rapid blood clearance combined with minimal urinary excretion. Both features yield clear advantages for local tumor assessment, as high radiopharmaceutical retention in the bladder and ureters is known to impair image interpretation.

102 patients with biochemical recurrent prostate cancer after RP were matched based on various clinical variables patients with corresponding [68Ga]Ga-PSMA-11 scans [136]. In doing so, fluorine-18-PSMA-1007 PET revealed approximately 5 times more lesions attributed to benign origin compared to [68Ga]Ga-PSMA-11 PET. Highest frequencies were observed in ganglia, unspecific lymph nodes and bone lesions with 43%, 31%, 24% with fluorine-18-PSMA-1007 and 29%, 42%, 27% with [68Ga]Ga-PSMA-11.

In addition to the number of detected lesions, the SUV_{max} of lesions attributed to benign origin was also significantly higher ($P<0.0001$) with [18F]F-PSMA-1007 PET (5.3 with a range of 3.0-42.7 vs. 4.4 with a range of 2.8-7.5 respectively). Further, a similar number of lesions was attributed to recurrent prostate cancer, 124/369 lesions for [18F]F-PSMA-1007 PET and 126/178 lesions for [68Ga]Ga-PSMA-11 PET. Therefore, in spite of key advantages, the considerable higher number of lesions with increased PSMA-ligand uptake attributed to benign lesions, as compared to [68Ga]Ga-PSMA-11 PET, emphasizes the need for paramount reader training and caution with [18F]F-PSMA-1007 as a prostate cancer imaging agent in the clinical context.

[68Ga]Ga-PSMA-11 vs. MRI

Multiparametric pelvic MRI is considered to be the standard imaging modality for staging and restaging local occurrence as well as for the detection of pelvic nodal metastases in prostate cancer patients. Several studies have assessed the respective performance of mpMRI and [68Ga]Ga-PSMA-11, including multiple PET/MRI hybrid studies.

Initial staging of patients with prostate cancer is paramount in the therapeutic decision-making. A number of studies [137-143] have assessed the diagnostic performance of [68Ga]Ga-PSMA-11 compared with conventional imaging in this context, especially for lymph node assessment and finally to evaluate management impact.

Comparison of [68Ga]Ga-PSMA-11 PET/CT with mpMRI for loco-regional prostate cancer staging in patients who were candidates for RP, using histopathology as reference standard, showed that PSMA PET/CT provided superior detection of prostate cancer lesions than mpMRI. For primary staging, another study focused on patients with high-risk prostate cancer, compared mpMRI combined with diffusion weighted whole body MRI to [68Ga]Ga-PSMA-11 imaging [144]. PET imaging allowed identifying nodal pelvic and extra-pelvic lesions as well as skeletal, liver and lung lesions that were not identified on MRI. However, the results obtained did not add value for T staging [144, 145]. Importantly, these results were counterbalanced by another study which found no significant differences between mpMRI and [68Ga]Ga-PSMA-11 for nodal staging in a series of 42 patients [146].

A side-by-side comparison of the diagnostic accuracy and inter-rater agreement of mpMRI and [68Ga]Ga-PSMA-11 PET/MRI for the detec-

tion of extracapsular extension and seminal vesicles infiltration was recently reported [145]. Both modalities performed equally for local staging of prostate cancer in patients with intermediate- to high-risk prostate cancer, since the slightly reduced specificity of [68Ga]Ga-PSMA-11 PET/MRI for the detection of extracapsular extension offset its increase in sensitivity.

When lesion volume estimate on imaging and histopathology were compared, both mpMRI and [68Ga]Ga-PSMA-11 PET showed good diagnostic performance, with a significant improvement when combining the areas identified as pathological on the two modalities [147, 148]. In the detection of local recurrence, mpMRI holds a significant advantage for local lesions over [68Ga]Ga-PSMA-11 PET, as excretion in the bladder reduces the aforementioned ability to detect focal uptake in the prostatic bed [149].

In the limited context of high-intensity focused ultrasound treatment of localized prostate cancer [150-153], patient follow-up typically includes mpMRI along with biopsy, which, in the post-interventional setting, often yields false-negative results. A study, aimed at investigating if [68Ga]Ga-PSMA-11 was used to localize recurrent disease in a cohort of 10 PET/MR patients with positive template biopsy and negative mpMRI after high-intensity focused ultrasound [154]. Predictive values of PET/MRI for sensitivity, specificity, and positive and negative were 55%, 100%, 100% and 85%, respectively. In addition, patient-based PET/MRI was negative in 40% of cases with Gleason scores 3 + 4 and a tumor length between 0.1 and 3 mm and all lesions with Gleason scores 4 + 3 or higher were detected on PET/MRI. Taken together, these results indicate that [68Ga]Ga-PSMA-11-PET/MR has the potential to localize prostate cancer recurrence after high-intensity focused ultrasound occult on mpMRI.

Whole body MRI is an emerging image modality for the detection of bone metastasis in patients with prostate cancer, mainly in case of bone marrow lesions, while sclerotic lesions might less visible [155]. However, for the detection of bone metastases [156, 157], the accuracy of [68Ga]Ga-PSMA-11 was shown to be significantly higher, with 100% vs. 80% [156] and 90% vs. 63% [157].

[68Ga]Ga-PSMA-11 vs. bone scan

Bone scanning, with [99mTc]Tc-labeled disphosphonates or [18F]F-NaF, is a reference imaging modality for the evaluation of bone metastases, namely in prostate cancer. The use of [68Ga]Ga-PSMA-11 imaging both in staging and restaging has shown an incidence of bone metastases higher than expected with conventional imaging on the basis of PSA levels and disease stage [158], motivating direct comparison studies with bone scan.

Multiple groups have consistently reported the superior diagnostic accuracy of [68Ga]Ga-PSMA-11 over technetium-99m-based bone scan [159, 160]. The comparison with fluorine-18-sodium fluoride, on the other hand, did not show a clear superiority of one modality over the other [161, 162], suggesting that the superior spatial resolution and sensitivity provided by the PET technology are a key factor in bone lesion detection.

As benign bone lesions might exhibit moderate [68Ga]Ga-PSMA-11 binding (see paragraph on false positive findings), reporting recommendations based on the absolute uptake value or relative uptake as compared with the physiologic uptake in other organs have been proposed [43, 163, 164].

Summary

From an imaging point of view, [68Ga]Ga-PSMA-11 PET/CT is unquestionably one of the most useful tools for the therapeutic management of patients with prostate cancer in the clinical setting in 2020 and foreseeable future. When compared with other imaging modalities, [68Ga]Ga-PSMA-11 targeted imaging appears to offer higher sensitivity along with higher levels of specificity as examplified in **Figure 5**. The sensitivity of radiopharmaceuticals targeting PSMA generally correlates positively with serum PSA levels, [68Ga]Ga-PSMA-11 PET/CT follows this pattern and performs relatively well at low PSA levels. Head-to-head comparisons with other molecular agents, such as [11C]-choline or [18F]F-PSMA-1007 in patients with biochemically recurrent prostate cancer, proved that [68Ga]Ga-PSMA-11 shows on-par or superior overall performance (**Figure 2** includes representative in-house images of head-to-head

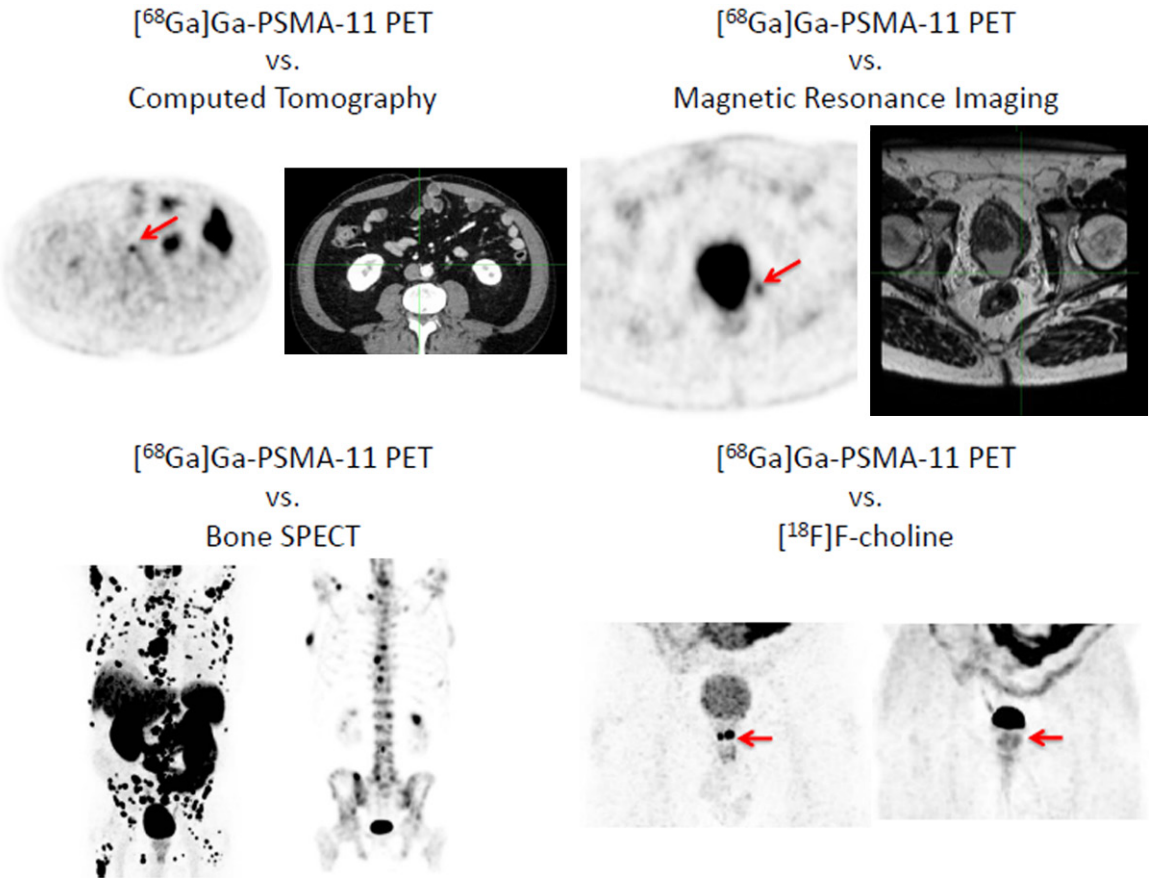

Figure 5. Upper panel left: [68Ga]Ga-PSMA-11 PET (left) vs. CT (right): Specific PSMA Uptake in a nodal recurrence in a millimetric size lymph node; Upper panel right: [68Ga]Ga-PSMA-11 PET vs. MRI: Specific PSMA Uptake not detected by MRI imaging. Lower panel left: [68Ga]Ga-PSMA-11 PET vs. technetium-99m-MDP SPECT performed 2 months apart, [68Ga]Ga-PSMA-11 PET shows a higher number of metastatic bone sites. Lower panel right: [68Ga]Ga-PSMA-11 PET vs. [11C]choline of a local recurrence.

direct comparisons of different imaging modalities or radiopharmaceuticals).

Other clinical applications of [68Ga]Ga-PSMA-11 imaging are already being considered, namely as imaging tool to guide targeted treatment. Intraprocedural detection of local [68Ga]Ga-PSMA-11 uptake might facilitate biopsies or surgery. Several studies [137, 140, 165-167] suggest that [68Ga]Ga-PSMA-11 PET/CT or PET/MRI guided prostate biopsy could have an added value, namely in patients with contraindications to or negative multi-parametric MRI and could contribute to the optimization of the diagnostic/therapeutic algorithm with benefits for patients. In addition, the in-situ detection of small sub-centimeter nodal metastases was reported during PSMA-radio-guided surgery, during which additional lesions, not detected with preoperative [68Ga]Ga-PSMA-11 PET/CT and close to known tumor deposits, were identified [168].

Dose escalated radiotherapy protocols have been demonstrated to improve the long-term biochemical control of prostate cancer patients. Focal boosts to the dominant intraprostatic lesion have been investigated as treatment strategy to improve disease control and optimize treatment-related side effects [169]. Noteworthy, complementary information in the definition of the target volume has been observed by IMRT dose escalation on the gross target volume based on the combination of mpMRI and [68Ga]Ga-PSMA-11 PET/CT imaging [170, 171]. Dose painting by boosting the gross target volume-union resulted in an estimated higher tumor control probability with no or minimal increase of normal tissue complication probability.

Last but not least, [68Ga]Ga-PSMA-11 PET has been shown to increase consensus with histopathology compared to mpMRI for intrapros-

tatic gross target volume delineation [172]. Therefore, use of [68Ga]Ga-PSMA-11 PET finds an interest in the treatment planning of salvage therapies for a local relapse after a primary radiotherapy [173], including PSMA-dose painting stereotactic radiotherapy to the intraprostatic focal recurrence.

Disclosure of conflict of interest

None.

Address correspondence to: Dr. Frédéric Bois, Division of Nuclear Medicine, University Hospital Geneva (HUG), 4, Rue Gabrielle-Perret-Gentil, CH-1211 Geneva 14, Geneva, Switzerland. Tel: +41 (0) 22 37 27587; Fax: +41 (0) 22 37 27184; E-mail: Frederic.Bois@hcuge.ch

References

[1] Bray F, Ferlay J, Soerjomataram I, Siegel RL, Torre LA and Jemal A. Global cancer statistics 2018: GLOBOCAN estimates of incidence and mortality worldwide for 36 cancers in 185 countries. CA Cancer J Clin 2018; 68: 394-424.

[2] (ONS) UsOfNS. 2018.

[3] Ilic D, Neuberger MM, Djulbegovic M and Dahm P. Screening for prostate cancer. Cochrane Database Syst Rev 2013; 31: CD004720.

[4] Loeb S. Guideline of guidelines: prostate cancer screening. BJU Int 2014; 114: 323-325.

[5] Sadi MV. PSA screening for prostate cancer. Rev Assoc Med Bras (1992) 2017; 63: 722-725.

[6] Nevedomskaya E, Baumgart SJ and Haendler B. Recent advances in prostate cancer treatment and drug discovery. Int J Mol Sci 2018; 19: 1359.

[7] Agarwal PK, Sadetsky N, Konety BR, Resnick MI and Carroll PR; Cancer of the Prostate Strategic Urological Research Endeavor (CaPSURE). Treatment failure after primary and salvage therapy for prostate cancer: likelihood, patterns of care, and outcomes. Cancer 2008; 112: 307-14.

[8] Pound CR, Partin AW, Eisenberger MA, Chan DW, Pearson JD and Walsh PC. Natural history of progression after PSA elevation following radical prostatectomy. JAMA 1999; 281: 1591-1597.

[9] Ang M, Rajcic B, Foreman D, Moretti K and O'Callaghan ME. Men presenting with prostate-specific antigen (PSA) values of over 100 ng/mL. BJU Int 2016; 117 Suppl 4: 68-75.

[10] Carvalhal GF, Smith DS, Mager DE, Ramos C and Catalona WJ. Digital rectal examination for detecting prostate cancer at prostate specific antigen levels of 4 ng/ml. or less. J Urol 1999; 161: 835-839.

[11] Cui T, Kovell RC and Terlecki RP. Is it time to abandon the digital rectal examination? Lessons from the PLCO cancer screening trial and peer-reviewed literature. Curr Med Res Opin 2016; 32: 1663-1669.

[12] Thompson IM, Pauler DK, Goodman PJ, Tangen CM, Lucia MS, Parnes HL, Minasian LM, Ford LG, Lippman SM, Crawford ED, Crowley JJ and Coltman CA Jr. Prevalence of prostate cancer among men with a prostate-specific antigen level < or =4.0 ng per milliliter. N Engl J Med 2004; 350: 2239-46.

[13] Hovels AM, Heesakkers RA, Adang EM, Jager GJ, Strum S, Hoogeveen YL, Severens JL and Barentsz JO. The diagnostic accuracy of CT and MRI in the staging of pelvic lymph nodes in patients with prostate cancer: a meta-analysis. Clin Radiol 2008; 63: 387-395.

[14] Radtke JP, Teber D, Hohenfellner M and Hadaschik BA. The current and future role of magnetic resonance imaging in prostate cancer detection and management. Transl Androl Urol 2015; 4: 326-341.

[15] Saokar A, Islam T, Jantsch M, Saksena MA, Hahn PF and Harisinghani MG. Detection of lymph nodes in pelvic malignancies with computed tomography and magnetic resonance imaging. Clin Imaging 2010; 34: 361-366.

[16] Rouviere O and Moldovan PC. The current role of prostate multiparametric magnetic resonance imaging. Asian J Urol 2019; 6: 137-145.

[17] Therasse P, Arbuck SG, Eisenhauer EA, Wanders J, Kaplan RS, Rubinstein L, Verweij J, Van Glabbeke M, van Oosterom AT, Christian MC and Gwyther SG. New guidelines to evaluate the response to treatment in solid tumors. European Organization for Research and Treatment of Cancer, National Cancer Institute of the United States, National Cancer Institute of Canada. J Natl Cancer Inst 2000; 92: 205-16.

[18] Yao V, Berkman CE, Choi JK, O'Keefe DS and Bacich DJ. Expression of prostate-specific membrane antigen (PSMA), increases cell folate uptake and proliferation and suggests a novel role for PSMA in the uptake of the non-polyglutamated folate, folic acid. Prostate 2010; 70: 305-316.

[19] Bouchelouche K, Turkbey B and Choyke PL. PSMA PET and radionuclide therapy in prostate cancer. Semin Nucl Med 2016; 46: 522-535.

[20] Birtle AJ, Freeman A, Masters JR, Payne HA and Harland SJ; BAUS Section of Oncology Cancer Registry. Tumour markers for managing men who present with metastatic prostate cancer and serum prostate-specific antigen levels of <10 ng/mL. BJU Int 2005; 96: 303-307.

[21] Rajasekaran AK, Anilkumar G and Christiansen JJ. Is prostate-specific membrane antigen a multifunctional protein? Am J Physiol Cell Physiol 2005; 288: C975-981.
[22] Silver DA, Pellicer I, Fair WR, Heston WD and Cordon-Cardo C. Prostate-specific membrane antigen expression in normal and malignant human tissues. Clin Cancer Res 1997; 3: 81-85.
[23] Rajasekaran SA, Anilkumar G, Oshima E, Bowie JU, Liu H, Heston W, Bander NH and Rajasekaran AK. A novel cytoplasmic tail MXXXL motif mediates the internalization of prostate-specific membrane antigen. Mol Biol Cell 2003; 14: 4835-4845.
[24] Chang SS. Overview of prostate-specific membrane antigen. Rev Urol 2004; 6 Suppl 10: S13-18.
[25] Mannweiler S, Amersdorfer P, Trajanoski S, Terrett JA, King D and Mehes G. Heterogeneity of prostate-specific membrane antigen (PSMA) expression in prostate carcinoma with distant metastasis. Pathol Oncol Res 2009; 15: 167-172.
[26] Fung EK, Cheal SM, Fareedy SB, Punzalan B, Beylergil V, Amir J, Chalasani S, Weber WA, Spratt DE, Veach DR, Bander NH, Larson SM, Zanzonico PB and Osborne JR. Targeting of radiolabeled J591 antibody to PSMA-expressing tumors: optimization of imaging and therapy based on non-linear compartmental modeling. EJNMMI Res 2016; 6: 7.
[27] Petronis JD, Regan F and Lin K. Indium-111 capromab pendetide (ProstaScint) imaging to detect recurrent and metastatic prostate cancer. Clin Nucl Med 1998; 23: 672-677.
[28] Sodee DB, Malguria N, Faulhaber P, Resnick MI, Albert J and Bakale G. Multicenter ProstaScint imaging findings in 2154 patients with prostate cancer. The ProstaScint imaging centers. Urology 2000; 56: 988-993.
[29] Deb N, Goris M, Trisler K, Fowler S, Saal J, Ning S, Becker M, Marquez C and Knox S. Treatment of hormone-refractory prostate cancer with 90Y-CYT-356 monoclonal antibody. Clin Cancer Res 1996; 2: 1289-1297.
[30] Pandit-Taskar N, O'Donoghue JA, Beylergil V, Lyashchenko S, Ruan S, Solomon SB, Durack JC, Carrasquillo JA, Lefkowitz RA, Gonen M, Lewis JS, Holland JP, Cheal SM, Reuter VE, Osborne JR, Loda MF, Smith-Jones PM, Weber WA, Bander NH, Scher HI, Morris MJ and Larson SM. (8)(9)Zr-huJ591 immuno-PET imaging in patients with advanced metastatic prostate cancer. Eur J Nucl Med Mol Imaging 2014; 41: 2093-2105.
[31] Tagawa ST, Milowsky MI, Morris M, Vallabhajosula S, Christos P, Akhtar NH, Osborne J, Goldsmith SJ, Larson S, Taskar NP, Scher HI, Bander NH and Nanus DM. Phase II study of Lutetium-177-labeled anti-prostate-specific membrane antigen monoclonal antibody J591 for metastatic castration-resistant prostate cancer. Clin Cancer Res 2013; 19: 5182-5191.
[32] Lutje S, Slavik R, Fendler W, Herrmann K and Eiber M. PSMA ligands in prostate cancer - probe optimization and theranostic applications. Methods 2017; 130: 42-50.
[33] Kozikowski AP, Nan F, Conti P, Zhang J, Ramadan E, Bzdega T, Wroblewska B, Neale JH, Pshenichkin S and Wroblewski JT. Design of remarkably simple, yet potent urea-based inhibitors of glutamate carboxypeptidase II (NAALADase). J Med Chem 2001; 44: 298-301.
[34] Eder M, Schafer M, Bauder-Wust U, Hull WE, Wangler C, Mier W, Haberkorn U and Eisenhut M. 68Ga-complex lipophilicity and the targeting property of a urea-based PSMA inhibitor for PET imaging. Bioconjug Chem 2012; 23: 688-697.
[35] Afshar-Oromieh A, Haberkorn U, Eder M, Eisenhut M and Zechmann CM. [68Ga]Gallium-labelled PSMA ligand as superior PET tracer for the diagnosis of prostate cancer: comparison with 18F-FECH. Eur J Nucl Med Mol Imaging 2012; 39: 1085-1086.
[36] Afshar-Oromieh A, Haberkorn U, Hadaschik B, Habl G, Eder M, Eisenhut M, Schlemmer HP and Roethke MC. PET/MRI with a 68Ga-PSMA ligand for the detection of prostate cancer. Eur J Nucl Med Mol Imaging 2013; 40: 1629-1630.
[37] Eder M, Eisenhut M, Babich J and Haberkorn U. PSMA as a target for radiolabelled small molecules. Eur J Nucl Med Mol Imaging 2013; 40: 819-823.
[38] Eder M, Neels O, Muller M, Bauder-Wust U, Remde Y, Schafer M, Hennrich U, Eisenhut M, Afshar-Oromieh A, Haberkorn U and Kopka K. Novel preclinical and radiopharmaceutical aspects of [68Ga]Ga-PSMA-HBED-CC: a new PET tracer for imaging of prostate cancer. Pharmaceuticals (Basel) 2014; 7: 779-796.
[39] Schuhmacher J, Klivenyi G, Matys R, Stadler M, Regiert T, Hauser H, Doll J, Maier-Borst W and Zoller M. Multistep tumor targeting in nude mice using bispecific antibodies and a gallium chelate suitable for immunoscintigraphy with positron emission tomography. Cancer Res 1995; 55: 115-123.
[40] Schuhmacher J, Klivenyi G, Hull WE, Matys R, Hauser H, Kalthoff H, Schmiegel WH, Maier-Borst W and Matzku S. A bifunctional HBED-derivative for labeling of antibodies with 67Ga, 111In and 59Fe. Comparative biodistribution with 111In-DPTA and 131I-labeled antibodies in mice bearing antibody internalizing and non-

internalizing tumors. Int J Rad Appl Instrum B 1992; 19: 809-824.
[41] Eder M, Knackmuss S, Le Gall F, Reusch U, Rybin V, Little M, Haberkorn U, Mier W and Eisenhut M. 68Ga-labelled recombinant antibody variants for immuno-PET imaging of solid tumours. Eur J Nucl Med Mol Imaging 2010; 37: 1397-1407.
[42] Luckerath K, Stuparu AD, Wei L, Kim W, Radu CG, Mona CE, Calais J, Rettig M, Reiter RE, Czernin J, Slavik R, Herrmann K, Eiber M and Fendler WP. Detection threshold and reproducibility of (68)Ga-PSMA11 PET/CT in a mouse model of prostate cancer. J Nucl Med 2018; 59: 1392-1397.
[43] Eiber M, Herrmann K, Calais J, Hadaschik B, Giesel FL, Hartenbach M, Hope T, Reiter R, Maurer T, Weber WA and Fendler WP. Prostate cancer molecular imaging standardized evaluation (promise): proposed miTNM Classification for the interpretation of PSMA-Ligand PET/CT. J Nucl Med 2018; 59: 469-478.
[44] Sandgren K, Johansson L, Axelsson J, Jonsson J, Ogren M, Ogren M, Andersson M, Strandberg S, Nyholm T, Riklund K and Widmark A. Radiation dosimetry of [(68)Ga]PSMA-11 in low-risk prostate cancer patients. EJNMMI Phys 2019; 6: 2.
[45] Fendler WP, Eiber M, Beheshti M, Bomanji J, Ceci F, Cho S, Giesel F, Haberkorn U, Hope TA, Kopka K, Krause BJ, Mottaghy FM, Schoder H, Sunderland J, Wan S, Wester HJ, Fanti S and Herrmann K. (68)Ga-PSMA PET/CT: joint EANM and SNMMI procedure guideline for prostate cancer imaging: version 1.0. Eur J Nucl Med Mol Imaging 2017; 44: 1014-1024.
[46] Rauscher I, Fendler WP, Hope T, Quon A, Nekolla SG, Calais J, Richter A, Haller B, Herrmann K, Weber WA, Czernin J and Eiber M. Can the injected dose be reduced in (68)Ga-PSMA-11 PET/CT maintaining high image quality for lesion detection? J Nucl Med 2019; 61: 189-193.
[47] Prasad V, Steffen IG, Diederichs G, Makowski MR, Wust P and Brenner W. Biodistribution of [(68)Ga]PSMA-HBED-CC in patients with prostate cancer: characterization of uptake in normal organs and tumour lesions. Mol Imaging Biol 2016; 18: 428-436.
[48] Klein Nulent TJW, Valstar MH, de Keizer B, Willems SM, Smit LA, Al-Mamgani A, Smeele LE, van Es RJJ, de Bree R and Vogel WV. Physiologic distribution of PSMA-ligand in salivary glands and seromucous glands of the head and neck on PET/CT. Oral Surg Oral Med Oral Pathol Oral Radiol 2018; 125: 478-486.
[49] van Kalmthout LWM, Lam M, de Keizer B, Krijger GC, Ververs TFT, de Roos R and Braat A. Impact of external cooling with icepacks on (68)Ga-PSMA uptake in salivary glands. EJNMMI Res 2018; 8: 56.
[50] Rupp NJ, Umbricht CA, Pizzuto DA, Lenggenhager D, Topfer A, Muller J, Muehlematter UJ, Ferraro DA, Messerli M, Morand GB, Huber GF, Eberli D, Schibli R, Muller C and Burger IA. First clinicopathologic evidence of a non-PSMA-related uptake mechanism for (68)Ga-PSMA-11 in salivary glands. J Nucl Med 2019; 60: 1270-1276.
[51] Krohn T, Verburg FA, Pufe T, Neuhuber W, Vogg A, Heinzel A, Mottaghy FM and Behrendt FF. [(68)Ga]PSMA-HBED uptake mimicking lymph node metastasis in coeliac ganglia: an important pitfall in clinical practice. Eur J Nucl Med Mol Imaging 2015; 42: 210-214.
[52] Beheshti M, Rezaee A and Langsteger W. 68Ga-PSMA-HBED uptake on cervicothoracic (Stellate) ganglia, a common pitfall on PET/CT. Clin Nucl Med 2017; 42: 195-196.
[53] Rischpler C, Beck TI, Okamoto S, Schlitter AM, Knorr K, Schwaiger M, Gschwend J, Maurer T, Meyer PT and Eiber M. (68)Ga-PSMA-HBED-CC uptake in cervical, coeliac and sacral ganglia as an important pitfall in prostate cancer PET imaging. J Nucl Med 2018; 59: 1406-1411.
[54] Ardies PJ, Gykiere P, Goethals L, De Mey J, De Geeter F and Everaert H. psma uptake in mediastinal sarcoidosis. Clin Nucl Med 2017; 42: 303-305.
[55] Dias AH, Holm Vendelbo M and Bouchelouche K. Prostate-specific membrane antigen PET/CT: uptake in lymph nodes with active sarcoidosis. Clin Nucl Med 2017; 42: e175-e176.
[56] Hermann RM, Djannatian M, Czech N and Nitsche M. Prostate-specific membrane antigen PET/CT: false-positive results due to sarcoidosis? Case Rep Oncol 2016; 9: 457-463.
[57] Kobe C, Maintz D, Fischer T, Drzezga A and Chang DH. Prostate-specific membrane antigen PET/CT in splenic sarcoidosis. Clin Nucl Med 2015; 40: 897-898.
[58] Foss CA, Mease RC, Cho SY, Kim HJ and Pomper MG. GCPII imaging and cancer. Curr Med Chem 2012; 19: 1346-1359.
[59] Gordon IO, Tretiakova MS, Noffsinger AE, Hart J, Reuter VE and Al-Ahmadie HA. Prostate-specific membrane antigen expression in regeneration and repair. Mod Pathol 2008; 21: 1421-1427.
[60] Artigas C, Otte FX, Lemort M, van Velthoven R and Flamen P. Vertebral hemangioma mimicking bone metastasis in 68Ga-PSMA ligand PET/CT. Clin Nucl Med 2017; 42: 368-370.
[61] Bhardwaj H, Stephens M, Bhatt M and Thomas PA. Prostate-specific membrane antigen PET/CT findings for hepatic hemangioma. Clin Nucl Med 2016; 41: 968-969.

[62] Jochumsen MR, Vendelbo MH, Hoyer S and Bouchelouche K. Subcutaneous lobular capillary hemangioma on 68Ga-PSMA PET/CT. Clin Nucl Med 2017; 42: e214-e215.
[63] De Coster L, Sciot R, Everaerts W, Gheysens O, Verscuren R, Deroose CM, Pans S, Van Laere K and Goffin KE. Fibrous dysplasia mimicking bone metastasis on (68)GA-PSMA PET/MRI. Eur J Nucl Med Mol Imaging 2017; 44: 1607-1608.
[64] Artigas C, Alexiou J, Garcia C, Wimana Z, Otte FX, Gil T, Van Velthoven R and Flamen P. Paget bone disease demonstrated on (68)Ga-PSMA ligand PET/CT. Eur J Nucl Med Mol Imaging 2016; 43: 195-196.
[65] Blazak JK and Thomas P. Paget disease: a potential pitfall in PSMA PET for prostate cancer. Clin Nucl Med 2016; 41: 699-700.
[66] Bourgeois S, Gykiere P, Goethals L, Everaert H and De Geeter FW. Aspecific uptake of 68GA-PSMA in paget disease of the bone. Clin Nucl Med 2016; 41: 877-878.
[67] Derlin T, Weiberg D and Sohns JM. Multitracer Molecular imaging of paget disease targeting bone remodeling, fatty acid metabolism, and psma expression on PET/CT. Clin Nucl Med 2016; 41: 991-992.
[68] Froehner M, Toma M, Zophel K, Novotny V, Laniado M and Wirth MP. PSMA-PET/CT-positive paget disease in a patient with newly diagnosed prostate cancer: imaging and bone biopsy findings. Case Rep Urol 2017; 2017: 1654231.
[69] Rowe SP, Deville C, Paller C, Cho SY, Fishman EK, Pomper MG, Ross AE and Gorin MA. Uptake of (18)F-DCFPyL in paget's disease of bone, an important potential pitfall in clinical interpretation of PSMA PET studies. Tomography 2015; 1: 81-84.
[70] Sasikumar A, Joy A, Nanabala R, Pillai MR and T AH. 68Ga-PSMA PET/CT false-positive tracer uptake in paget disease. Clin Nucl Med 2016; 41: e454-455.
[71] Gykiere P, Goethals L and Everaert H. Healing sacral fracture masquerading as metastatic bone disease on a 68Ga-PSMA PET/CT. Clin Nucl Med 2016; 41: e346-347.
[72] Vamadevan S, Le K, Bui C and Mansberg R. Incidental PSMA uptake in an undisplaced fracture of a vertebral body. Clin Nucl Med 2017; 42: 465-466.
[73] Pyka T, Weirich G, Einspieler I, Maurer T, Theisen J, Hatzichristodoulou G, Schwamborn K, Schwaiger M and Eiber M. 68Ga-PSMA-HBED-CC PET for Differential diagnosis of suggestive lung lesions in patients with prostate cancer. J Nucl Med 2016; 57: 367-371.
[74] Bilgin R, Ergul N and Cermik TF. Incidental meningioma mimicking metastasis of prostate adenocarcinoma in 68Ga-Labeled PSMA ligand PET/CT. Clin Nucl Med 2016; 41: 956-958.
[75] Jain TK, Jois AG, Kumar VS, Singh SK, Kumar R and Mittal BR. Incidental detection of tracer avidity in meningioma in (68)Ga-PSMA PET/CT during initial staging for prostate cancer. Rev Esp Med Nucl Imagen Mol 2017; 36: 133-134.
[76] Kanthan GL, Izard MA, Emmett L, Hsiao E and Schembri GP. Schwannoma showing avid uptake on 68Ga-PSMA-HBED-CC PET/CT. Clin Nucl Med 2016; 41: 703-704.
[77] Rischpler C, Maurer T, Schwaiger M and Eiber M. Intense PSMA-expression using (68)Ga-PSMA PET/CT in a paravertebral schwannoma mimicking prostate cancer metastasis. Eur J Nucl Med Mol Imaging 2016; 43: 193-194.
[78] Vamadevan S, Le K, Shen L, Ha L and Mansberg R. Incidental prostate-specific membrane antigen uptake in a peripheral nerve sheath tumor. Clin Nucl Med 2017; 42: 560-562.
[79] Chan M and Hsiao E. Subacute cortical infarct showing uptake on 68Ga-PSMA PET/CT. Clin Nucl Med 2017; 42: 110-111.
[80] Noto B, Vrachimis A, Schafers M, Stegger L and Rahbar K. Subacute stroke mimicking cerebral metastasis in 68Ga-PSMA-HBED-CC PET/CT. Clin Nucl Med 2016; 41: e449-451.
[81] Henninger M, Maurer T, Hacker C and Eiber M. 68Ga-PSMA PET/MR showing intense PSMA uptake in nodular fasciitis mimicking prostate cancer metastasis. Clin Nucl Med 2016; 41: e443-444.
[82] Malik D, Basher RK, Mittal BR, Jain TK, Bal A and Singh SK. 68Ga-PSMA expression in pseudoangiomatous stromal hyperplasia of the breast. Clin Nucl Med 2017; 42: 58-60.
[83] Zacho HD, Nielsen JB, Dettmann K, Hjulskov SH and Petersen LJ. 68Ga-PSMA PET/CT uptake in Intramuscular myxoma imitates prostate cancer metastasis. Clin Nucl Med 2017; 42: 487-488.
[84] Kanthan GL, Hsiao E, Kneebone A, Eade T and Schembri GP. Desmoid tumor showing intense uptake on 68Ga PSMA-HBED-CC PET/CT. Clin Nucl Med 2016; 41: 508-509.
[85] Daglioz Gorur G, Hekimsoy T, Isgoren S, Sikar Akturk A and Demir H. Uptake of an acrochordon incidentally detected on 68Ga prostate-specific membrane antigen PET/CT. Clin Nucl Med 2017; 42: 461-462.
[86] Aydin F, Akcal A, Unal B, Sezgin Goksu S and Gungor F. 68Ga-PSMA uptake by dermatofibroma in a patient with prostate cancer. Clin Nucl Med 2017; 42: 358-360.
[87] Bostwick DG, Pacelli A, Blute M, Roche P and Murphy GP. Prostate specific membrane antigen expression in prostatic intraepithelial neoplasia and adenocarcinoma: a study of 184 cases. Cancer 1998; 82: 2256-2261.

[88] Woythal N, Arsenic R, Kempkensteffen C, Miller K, Janssen JC, Huang K, Makowski MR, Brenner W and Prasad V. Immunohistochemical validation of PSMA expression measured by (68)Ga-PSMA PET/CT in primary prostate cancer. J Nucl Med 2018; 59: 238-243.

[89] Chakraborty PS, Tripathi M, Agarwal KK, Kumar R, Vijay MK and Bal C. Metastatic poorly differentiated prostatic carcinoma with neuroendocrine differentiation: negative on 68Ga-PSMA PET/CT. Clin Nucl Med 2015; 40: e163-166.

[90] Tosoian JJ, Gorin MA, Rowe SP, Andreas D, Szabo Z, Pienta KJ, Pomper MG, Lotan TL and Ross AE. Correlation of PSMA-targeted (18)F-DCFPyL PET/CT findings with immunohistochemical and genomic data in a patient with metastatic neuroendocrine prostate cancer. Clin Genitourin Cancer 2017; 15: e65-e68.

[91] Usmani S, Ahmed N, Marafi F, Rasheed R, Amanguno HG and Al Kandari F. Molecular imaging in neuroendocrine differentiation of prostate cancer: 68Ga-PSMA versus 68Ga-DOTA NOC PET-CT. Clin Nucl Med 2017; 42: 410-413.

[92] Sweat SD, Pacelli A, Murphy GP and Bostwick DG. Prostate-specific membrane antigen expression is greatest in prostate adenocarcinoma and lymph node metastases. Urology 1998; 52: 637-640.

[93] Ristau BT, O'Keefe DS and Bacich DJ. The prostate-specific membrane antigen: lessons and current clinical implications from 20 years of research. Urol Oncol 2014; 32: 272-279.

[94] Rowe SP, Gorin MA, Salas Fragomeni RA, Drzezga A and Pomper MG. Clinical experience with (18)F-labeled small molecule inhibitors of prostate-specific membrane antigen. PET Clin 2017; 12: 235-241.

[95] Demirci E, Ocak M, Kabasakal L, Decristoforo C, Talat Z, Halac M and Kanmaz B. (68)Ga-PSMA PET/CT imaging of metastatic clear cell renal cell carcinoma. Eur J Nucl Med Mol Imaging 2014; 41: 1461-1462.

[96] Gorin MA, Rowe SP, Hooper JE, Kates M, Hammers HJ, Szabo Z, Pomper MG and Allaf ME. PSMA-targeted (18)F-DCFPyL PET/CT imaging of clear cell renal cell carcinoma: results from a rapid autopsy. Eur Urol 2017; 71: 145-146.

[97] Joshi A, Nicholson C, Rhee H, Gustafson S, Miles K and Vela I. Incidental malignancies identified during staging for prostate cancer with (68)Ga prostate-specific membrane antigen HBED-CC positron emission tomography imaging. Urology 2017; 104: e3-e4.

[98] Rhee H, Blazak J, Tham CM, Ng KL, Shepherd B, Lawson M, Preston J, Vela I, Thomas P and Wood S. Pilot study: use of gallium-68 PSMA PET for detection of metastatic lesions in patients with renal tumour. EJNMMI Res 2016; 6: 76.

[99] Rowe SP, Gorin MA, Hammers HJ, Pomper MG, Allaf ME and Javadi MS. Detection of 18F-FDG PET/CT occult lesions with 18F-DCFPyL PET/CT in a patient with metastatic renal cell carcinoma. Clin Nucl Med 2016; 41: 83-85.

[100] Rowe SP, Gorin MA, Hammers HJ, Som Javadi M, Hawasli H, Szabo Z, Cho SY, Pomper MG and Allaf ME. Imaging of metastatic clear cell renal cell carcinoma with PSMA-targeted (1)(8) F-DCFPyL PET/CT. Ann Nucl Med 2015; 29: 877-882.

[101] Sasikumar A, Joy A, Nanabala R, Unni M and Tk P. Complimentary pattern of uptake in 18F-FDG PET/CT and 68Ga-prostate-specific membrane antigen PET/CT in a case of metastatic clear cell renal carcinoma. Clin Nucl Med 2016; 41: e517-e519.

[102] Sawicki LM, Buchbender C, Boos J, Giessing M, Ermert J, Antke C, Antoch G and Hautzel H. Diagnostic potential of PET/CT using a (68)Ga-labelled prostate-specific membrane antigen ligand in whole-body staging of renal cell carcinoma: initial experience. Eur J Nucl Med Mol Imaging 2017; 44: 102-107.

[103] Al-Ahmadie HA, Olgac S, Gregor PD, Tickoo SK, Fine SW, Kondagunta GV, Scher HI, Morris MJ, Russo P, Motzer RJ and Reuter VE. Expression of prostate-specific membrane antigen in renal cortical tumors. Mod Pathol 2008; 21: 727-732.

[104] Sheikhbahaei S, Afshar-Oromieh A, Eiber M, Solnes LB, Javadi MS, Ross AE, Pienta KJ, Allaf ME, Haberkorn U, Pomper MG, Gorin MA and Rowe SP. Pearls and pitfalls in clinical interpretation of prostate-specific membrane antigen (PSMA)-targeted PET imaging. Eur J Nucl Med Mol Imaging 2017; 44: 2117-2136.

[105] Guidelines PC. EAU EANM ESTRO ESUR SIOG guidelines on prostate cancer. 2019.

[106] von Eyben FE, Picchio M, von Eyben R, Rhee H and Bauman G. (68)Ga-labeled prostate-specific membrane antigen ligand positron emission tomography/computed tomography for prostate Cancer: a systematic review and meta-analysis. Eur Urol Focus 2018; 4: 686-693.

[107] Perera M, Papa N, Christidis D, Wetherell D, Hofman MS, Murphy DG, Bolton D and Lawrentschuk N. Sensitivity, specificity, and predictors of positive (68)Ga-prostate-specific membrane antigen positron emission tomography in advanced prostate cancer: a systematic review and meta-analysis. Eur Urol 2016; 70: 926-937.

[108] Muller J, Ferraro DA, Muehlematter UJ, Garcia Schuler HI, Kedzia S, Eberli D, Guckenberger M, Kroeze SGC, Sulser T, Schmid DM, Omlin A, Muller A, Zilli T, John H, Kranzbuehler H,

Kaufmann PA, von Schulthess GK and Burger IA. Clinical impact of (68)Ga-PSMA-11 PET on patient management and outcome, including all patients referred for an increase in PSA level during the first year after its clinical introduction. Eur J Nucl Med Mol Imaging 2019; 46: 889-900.

[109] Fendler WP, Calais J, Eiber M, Flavell RR, Mishoe A, Feng FY, Nguyen HG, Reiter RE, Rettig MB, Okamoto S, Emmett L, Zacho HD, Ilhan H, Wetter A, Rischpler C, Schoder H, Burger IA, Gartmann J, Smith R, Small EJ, Slavik R, Carroll PR, Herrmann K, Czernin J and Hope TA. Assessment of 68Ga-PSMA-11 PET accuracy in localizing recurrent prostate cancer: a prospective single-arm clinical trial. JAMA Oncol 2019; 5: 856-863.

[110] Pfister D, Porres D, Heidenreich A, Heidegger I, Knuechel R, Steib F, Behrendt FF and Verburg FA. Detection of recurrent prostate cancer lesions before salvage lymphadenectomy is more accurate with (68)Ga-PSMA-HBED-CC than with (18)F-Fluoroethylcholine PET/CT. Eur J Nucl Med Mol Imaging 2016; 43: 1410-1417.

[111] Jilg CA, Drendel V, Rischke HC, Beck T, Vach W, Schaal K, Wetterauer U, Schultze-Seemann W and Meyer PT. Diagnostic accuracy of Ga-68-HBED-CC-PSMA-ligand-PET/CT before salvage lymph node dissection for recurrent prostate cancer. Theranostics 2017; 7: 1770-1780.

[112] Ceci F, Bianchi L, Borghesi M, Polverari G, Farolfi A, Briganti A, Schiavina R, Brunocilla E, Castellucci P and Fanti S. Prediction nomogram for (68)Ga-PSMA-11 PET/CT in different clinical settings of PSA failure after radical treatment for prostate cancer. Eur J Nucl Med Mol Imaging 2020; 47: 136-146.

[113] Calais J, Czernin J, Cao M, Kishan AU, Hegde JV, Shaverdian N, Sandler K, Chu FI, King CR, Steinberg ML, Rauscher I, Schmidt-Hegemann NS, Poeppel T, Hetkamp P, Ceci F, Herrmann K, Fendler WP, Eiber M and Nickols NG. (68)Ga-PSMA-11 PET/CT mapping of prostate cancer biochemical recurrence after radical prostatectomy in 270 patients with a PSA level of less than 1.0 ng/mL: impact on salvage radiotherapy planning. J Nucl Med 2018; 59: 230-237.

[114] Koerber SA, Will L, Kratochwil C, Haefner MF, Rathke H, Kremer C, Merkle J, Herfarth K, Kopka K, Choyke PL, Holland-Letz T, Haberkorn U, Debus J and Giesel FL. (68)Ga-PSMA-11 PET/CT in primary and recurrent prostate carcinoma: implications for radiotherapeutic management in 121 patients. J Nucl Med 2018; 60: 234-240.

[115] Boreta L, Gadzinski AJ, Wu SY, Xu M, Greene K, Quanstrom K, Nguyen HG, Carroll PR, Hope TA and Feng FY. Location of recurrence by Gallium-68 PSMA-11 PET scan in prostate cancer patients eligible for salvage radiotherapy. Urology 2019; 129: 165-171.

[116] Zilli T, Jorcano S, Peguret N, Caparrotti F, Hidalgo A, Khan HG, Vees H, Weber DC and Miralbell R. Dose-adapted salvage radiotherapy after radical prostatectomy based on an erMRI target definition model: toxicity analysis. Acta Oncol 2014; 53: 96-102.

[117] Tran S, Jorcano S, Falco T, Lamanna G, Miralbell R and Zilli T. Oligorecurrent nodal prostate cancer: long-term results of an elective nodal irradiation approach. Am J Clin Oncol 2018; 41: 960-962.

[118] Steuber T, Jilg C, Tennstedt P, De Bruycker A, Tilki D, Decaestecker K, Zilli T, Jereczek-Fossa BA, Wetterauer U, Grosu AL, Schultze-Seemann W, Heinzer H, Graefen M, Morlacco A, Karnes RJ and Ost P. Standard of care versus metastases-directed therapy for PET-detected nodal oligorecurrent prostate cancer following multimodality treatment: a multi-institutional case-control study. Eur Urol Focus 2019; 5: 1007-1013.

[119] Deek MP and Tran PT. Oligometastatic and oligoprogression disease and local therapies in prostate cancer. Cancer J 2020; 26: 137-143.

[120] Han S, Woo S, Kim YJ and Suh CH. Impact of (68)Ga-PSMA PET on the management of patients with prostate cancer: a systematic review and meta-analysis. Eur Urol 2018; 74: 179-190.

[121] Calais J, Czernin J, Fendler WP, Elashoff D and Nickols NG. Randomized prospective phase III trial of (68)Ga-PSMA-11 PET/CT molecular imaging for prostate cancer salvage radiotherapy planning [PSMA-SRT]. BMC Cancer 2019; 19: 18.

[122] Hope TA, Goodman JZ, Allen IE, Calais J, Fendler WP and Carroll PR. Metaanalysis of (68)Ga-PSMA-11 PET accuracy for the detection of prostate cancer validated by histopathology. J Nucl Med 2019; 60: 786-793.

[123] Hirmas N, Al-Ibraheem A, Herrmann K, Alsharif A, Muhsin H, Khader J, Al-Daghmin A and Salah S. [(68)Ga]PSMA PET/CT improves initial staging and management plan of patients with high-risk prostate cancer. Mol Imaging Biol 2019; 21: 574-581.

[124] Grubmuller B, Baltzer P, Hartenbach S, D'Andrea D, Helbich TH, Haug AR, Goldner GM, Wadsak W, Pfaff S, Mitterhauser M, Balber T, Berroteran-Infante N, Grahovac M, Babich J, Seitz C, Kramer G, Susani M, Mazal P, Kenner L, Shariat SF, Hacker M and Hartenbach M. PSMA ligand PET/MRI for primary prostate cancer: staging performance and clinical impact. Clin Cancer Res 2018; 24: 6300-6307.

[125] Parker CC, James ND, Brawley CD, Clarke NW, Hoyle AP, Ali A, Ritchie AWS, Attard G, Chowd-

hury S, Cross W, Dearnaley DP, Gillessen S, Gilson C, Jones RJ, Langley RE, Malik ZI, Mason MD, Matheson D, Millman R, Russell JM, Thalmann GN, Amos CL, Alonzi R, Bahl A, Birtle A, Din O, Douis H, Eswar C, Gale J, Gannon MR, Jonnada S, Khaksar S, Lester JF, O'Sullivan JM, Parikh OA, Pedley ID, Pudney DM, Sheehan DJ, Srihari NN, Tran ATH, Parmar MKB and Sydes MR; Systemic Therapy for Advanced or Metastatic Prostate cancer: Evaluation of Drug Efficacy (STAMPEDE) investigators. Radiotherapy to the primary tumour for newly diagnosed, metastatic prostate cancer (STAMPEDE): a randomised controlled phase 3 trial. Lancet 2018; 392: 2353-2366.

[126] Afshar-Oromieh A, Zechmann CM, Malcher A, Eder M, Eisenhut M, Linhart HG, Holland-Letz T, Hadaschik BA, Giesel FL, Debus J and Haberkorn U. Comparison of PET imaging with a (68)Ga-labelled PSMA ligand and (18)F-choline-based PET/CT for the diagnosis of recurrent prostate cancer. Eur J Nucl Med Mol Imaging 2014; 41: 11-20.

[127] Bluemel C, Krebs M, Polat B, Linke F, Eiber M, Samnick S, Lapa C, Lassmann M, Riedmiller H, Czernin J, Rubello D, Bley T, Kropf S, Wester HJ, Buck AK and Herrmann K. 68Ga-PSMA-PET/CT in Patients With Biochemical Prostate Cancer Recurrence and Negative 18F-Choline-PET/CT. Clin Nucl Med 2016; 41: 515-521.

[128] Morigi JJ, Stricker PD, van Leeuwen PJ, Tang R, Ho B, Nguyen Q, Hruby G, Fogarty G, Jagavkar R, Kneebone A, Hickey A, Fanti S, Tarlinton L and Emmett L. Prospective comparison of 18F-fluoromethylcholine versus 68Ga-PSMA PET/CT in prostate cancer patients who have rising psa after curative treatment and are being considered for targeted therapy. J Nucl Med 2015; 56: 1185-1190.

[129] Schwenck J, Rempp H, Reischl G, Kruck S, Stenzl A, Nikolaou K, Pfannenberg C and la Fougere C. Comparison of (68)Ga-labelled PSMA-11 and (11)C-choline in the detection of prostate cancer metastases by PET/CT. Eur J Nucl Med Mol Imaging 2017; 44: 92-101.

[130] Dietlein M, Kobe C, Kuhnert G, Stockter S, Fischer T, Schomacker K, Schmidt M, Dietlein F, Zlatopolskiy BD, Krapf P, Richarz R, Neubauer S, Drzezga A and Neumaier B. Comparison of [(18)F]DCFPyL and [(68)Ga]Ga-PSMA-HBED-CC for PSMA-PET imaging in patients with relapsed prostate cancer. Mol Imaging Biol 2015; 17: 575-584.

[131] Pernthaler B, Kulnik R, Gstettner C, Salamon S, Aigner RM and Kvaternik H. A prospective head-to-head comparison of 18f-fluciclovine with 68Ga-PSMA-11 in biochemical recurrence of prostate cancer in PET/CT. Clin Nucl Med 2019; 44: e566-e573.

[132] Calais J, Fendler WP, Herrmann K, Eiber M and Ceci F. Comparison of (68)Ga-PSMA-11 and (18)F-Fluciclovine PET/CT in a case series of 10 patients with prostate cancer recurrence. J Nucl Med 2018; 59: 789-794.

[133] Calais J, Ceci F, Eiber M, Hope TA, Hofman MS, Rischpler C, Bach-Gansmo T, Nanni C, Savir-Baruch B, Elashoff D, Grogan T, Dahlbom M, Slavik R, Gartmann J, Nguyen K, Lok V, Jadvar H, Kishan AU, Rettig MB, Reiter RE, Fendler WP and Czernin J. (18)F-fluciclovine PET-CT and (68)Ga-PSMA-11 PET-CT in patients with early biochemical recurrence after prostatectomy: a prospective, single-centre, single-arm, comparative imaging trial. Lancet Oncol 2019; 20: 1286-1294.

[134] Denes G. Comparison of 68Ga-PSMA-11 and 18F-Fluciclovine PET/CT in a case series of 10 patients with prostate cancer recurrence: interesting, but far from definitive. J Nucl Med 2018; 59: 860.

[135] Samir T. Re: 18F-Fluciclovine PET-CT and 68Ga-PSMA-11 PET-CT in patients with early biochemical recurrence after prostatectomy: a prospective, single-centre, single-arm, comparative imaging trial. J Urol 2020; 203: 661-662.

[136] Rauscher I, Kronke M, Konig M, Gafita A, Maurer T, Horn T, Schiller K, Weber WA and Eiber M. Matched-pair comparison of (68)Ga-PSMA-11 and (18)F-PSMA-1007 PET/CT: frequency of pitfalls and detection efficacy in biochemical recurrence after radical prostatectomy. J Nucl Med 2019; 61: 51-57

[137] Berger I, Annabattula C, Lewis J, Shetty DV, Kam J, Maclean F, Arianayagam M, Canagasingham B, Ferguson R, Khadra M, Ko R, Winter M, Loh H and Varol C. (68)Ga-PSMA PET/CT vs. mpMRI for locoregional prostate cancer staging: correlation with final histopathology. Prostate Cancer Prostatic Dis 2018; 21: 204-211.

[138] Giesel FL, Hadaschik B, Cardinale J, Radtke J, Vinsensia M, Lehnert W, Kesch C, Tolstov Y, Singer S, Grabe N, Duensing S, Schafer M, Neels OC, Mier W, Haberkorn U, Kopka K and Kratochwil C. F-18 labelled PSMA-1007: biodistribution, radiation dosimetry and histopathological validation of tumor lesions in prostate cancer patients. Eur J Nucl Med Mol Imaging 2017; 44: 678-688.

[139] Herlemann A, Wenter V, Kretschmer A, Thierfelder KM, Bartenstein P, Faber C, Gildehaus FJ, Stief CG, Gratzke C and Fendler WP. (68)Ga-PSMA positron emission tomography/computed tomography provides accurate staging of lymph node regions prior to lymph node dissection in patients with prostate cancer. Eur Urol 2016; 70: 553-557.

[140] Lopci E, Saita A, Lazzeri M, Lughezzani G, Colombo P, Buffi NM, Hurle R, Marzo K, Peschechera R, Benetti A, Zandegiacomo S, Pasini L, Lista G, Cardone P, Castello A, Maffei D, Balzarini L, Chiti A, Guazzoni G and Casale P. (68) Ga-PSMA positron emission tomography/computerized tomography for primary diagnosis of prostate cancer in men with contraindications to or negative multiparametric magnetic resonance imaging: a prospective observational study. J Urol 2018; 200: 95-103.

[141] Maurer T, Gschwend JE, Rauscher I, Souvatzoglou M, Haller B, Weirich G, Wester HJ, Heck M, Kubler H, Beer AJ, Schwaiger M and Eiber M. Diagnostic efficacy of (68)gallium-PSMA positron emission tomography compared to conventional imaging for lymph node staging of 130 consecutive patients with intermediate to high risk prostate cancer. J Urol 2016; 195: 1436-1443.

[142] Mottaghy FM, Heinzel A and Verburg FA. Molecular imaging using PSMA PET/CT versus multiparametric MRI for initial staging of prostate cancer: comparing apples with oranges? Eur J Nucl Med Mol Imaging 2016; 43: 1397-1399.

[143] van Leeuwen PJ, Emmett L, Ho B, Delprado W, Ting F, Nguyen Q and Stricker PD. Prospective evaluation of 68Gallium-prostate-specific membrane antigen positron emission tomography/computed tomography for preoperative lymph node staging in prostate cancer. BJU Int 2017; 119: 209-215.

[144] Tulsyan S, Das CJ, Tripathi M, Seth A, Kumar R and Bal C. Comparison of 68Ga-PSMA PET/CT and multiparametric MRI for staging of high-risk prostate cancer68Ga-PSMA PET and MRI in prostate cancer. Nucl Med Commun 2017; 38: 1094-1102.

[145] Muehlematter UJ, Burger IA, Becker AS, Schawkat K, Hotker AM, Reiner CS, Muller J, Rupp NJ, Ruschoff JH, Eberli D and Donati OF. Diagnostic accuracy of multiparametric MRI versus (68)Ga-PSMA-11 PET/MRI for extracapsular extension and seminal vesicle invasion in patients with prostate cancer. Radiology 2019; 293: 350-358.

[146] Zhang Q, Zang S, Zhang C, Fu Y, Lv X, Zhang Q, Deng Y, Zhang C, Luo R, Zhao X, Wang W, Wang F and Guo H. Comparison of (68)Ga-PSMA-11 PET-CT with mpMRI for preoperative lymph node staging in patients with intermediate to high-risk prostate cancer. J Transl Med 2017; 15: 230.

[147] Al-Bayati M, Grueneisen J, Lutje S, Sawicki LM, Suntharalingam S, Tschirdewahn S, Forsting M, Rubben H, Herrmann K, Umutlu L and Wetter A. Integrated 68Gallium labelled prostate-specific membrane antigen-11 positron emission tomography/magnetic resonance imaging enhances discriminatory power of multi-parametric prostate magnetic resonance imaging. Urol Int 2018; 100: 164-171.

[148] Zamboglou C, Drendel V, Jilg CA, Rischke HC, Beck TI, Schultze-Seemann W, Krauss T, Mix M, Schiller F, Wetterauer U, Werner M, Langer M, Bock M, Meyer PT and Grosu AL. Comparison of (68)Ga-HBED-CC PSMA-PET/CT and multiparametric MRI for gross tumour volume detection in patients with primary prostate cancer based on slice by slice comparison with histopathology. Theranostics 2017; 7: 228-237.

[149] Freitag MT, Radtke JP, Afshar-Oromieh A, Roethke MC, Hadaschik BA, Gleave M, Bonekamp D, Kopka K, Eder M, Heusser T, Kachelriess M, Wieczorek K, Sachpekidis C, Flechsig P, Giesel F, Hohenfellner M, Haberkorn U, Schlemmer HP and Dimitrakopoulou-Strauss A. Local recurrence of prostate cancer after radical prostatectomy is at risk to be missed in (68) Ga-PSMA-11-PET of PET/CT and PET/MRI: comparison with mpMRI integrated in simultaneous PET/MRI. Eur J Nucl Med Mol Imaging 2017; 44: 776-787.

[150] Apfelbeck M, Chaloupka M, Schlenker B, Stief CG and Clevert DA. Follow-up after focal therapy of the prostate with high intensity focused ultrasound (HIFU) using contrast enhanced ultrasound (CEUS) in combination with MRI image fusion. Clin Hemorheol Microcirc 2019; 73: 135-143.

[151] Hostiou T, Gelet A, Chapelon JY, Rouviere O, Mege-Lechevalier F, Lafon C, Tonoli-Catez H, Badet L and Crouzet S. Salvage high-intensity focused ultrasound for locally recurrent prostate cancer after low-dose-rate brachytherapy: oncological and functional outcomes. BJU Int 2019; 124: 746-757.

[152] Rosenhammer B, Niessen C, Rotzinger L, Reiss J, Schnabel MJ, Burger M and Brundl J. Oncological outcome and value of postoperative magnetic resonance imaging after focal high-intensity focused ultrasound therapy for prostate cancer. Urol Int 2019; 103: 270-278.

[153] Schmid FA, Schindele D, Mortezavi A, Spitznagel T, Sulser T, Schostak M and Eberli D. Prospective multicentre study using high intensity focused ultrasound (HIFU) for the focal treatment of prostate cancer: safety outcomes and complications. Urol Oncol 2020; 38: 225-230.

[154] Burger IA, Muller J, Donati OF, Ferraro DA, Messerli M, Kranzbuhler B, Ter Voert E, Muehlematter UJ, Rupp NJ, Mortezavi A and Eberli D. (68) Ga-PSMA-11 PET/MR detects local recurrence occult on mpmri in prostate cancer patients after HIFU. J Nucl Med 2019; 60: 1118-1123.

[155] Padhani AR, Koh DM and Collins DJ. Whole-body diffusion-weighted MR imaging in cancer: current status and research directions. Radiology 2011; 261: 700-718.

[156] Dyrberg E, Hendel HW, Huynh THV, Klausen TW, Logager VB, Madsen C, Pedersen EM, Pedersen M and Thomsen HS. (68)Ga-PSMA-PET/CT in comparison with (18)F-fluoride-PET/CT and whole-body MRI for the detection of bone metastases in patients with prostate cancer: a prospective diagnostic accuracy study. Eur Radiol 2019; 29: 1221-1230.

[157] Zacho HD, Nielsen JB, Afshar-Oromieh A, Haberkorn U, deSouza N, De Paepe K, Dettmann K, Langkilde NC, Haarmark C, Fisker RV, Arp DT, Carl J, Jensen JB and Petersen LJ. Prospective comparison of (68)Ga-PSMA PET/CT, (18)F-sodium fluoride PET/CT and diffusion weighted-MRI at for the detection of bone metastases in biochemically recurrent prostate cancer. Eur J Nucl Med Mol Imaging 2018; 45: 1884-1897.

[158] Pomykala KL, Czernin J, Grogan TR, Armstrong WR, Willliams J and Calais J. Total-body (68)Ga-PSMA-11 PET/CT for bone metastasis detection in prostate cancer patients: Potential impact on bone scan guidelines. J Nucl Med 2020; 61: 405-411.

[159] Pyka T, Okamoto S, Dahlbender M, Tauber R, Retz M, Heck M, Tamaki N, Schwaiger M, Maurer T and Eiber M. Comparison of bone scintigraphy and (68)Ga-PSMA PET for skeletal staging in prostate cancer. Eur J Nucl Med Mol Imaging 2016; 43: 2114-2121.

[160] Lengana T, Lawal IO, Boshomane TG, Popoola GO, Mokoala KMG, Moshokoa E, Maes A, Mokgoro NP, Van de Wiele C, Vorster M and Sathekge MM. (68)Ga-PSMA PET/CT replacing bone scan in the initial staging of skeletal metastasis in prostate cancer: a fait accompli? Clin Genitourin Cancer 2018; 16: 392-401.

[161] Zhou J, Gou Z, Wu R, Yuan Y, Yu G and Zhao Y. Comparison of PSMA-PET/CT, choline-PET/CT, NaF-PET/CT, MRI, and bone scintigraphy in the diagnosis of bone metastases in patients with prostate cancer: a systematic review and meta-analysis. Skeletal Radiol 2019; 48: 1915-1924.

[162] Uprimny C, Svirydenka A, Fritz J, Kroiss AS, Nilica B, Decristoforo C, Haubner R, von Guggenberg E, Buxbaum S, Horninger W and Virgolini IJ. Comparison of [(68)Ga]Ga-PSMA-11 PET/CT with [(18)F]NaF PET/CT in the evaluation of bone metastases in metastatic prostate cancer patients prior to radionuclide therapy. Eur J Nucl Med Mol Imaging 2018; 45: 1873-1883.

[163] Chiu LW, Lawhn-Heath C, Behr S, Juarez R, Perez PM, Lobach I, Bucknor MD, Hope TA and Flavell RR. Factors predicting metastatic disease in (68)Ga-PSMA-11 PET positive osseous lesions in prostate cancer. J Nucl Med 2020; [Epub ahead of print]

[164] Rowe SP, Pienta KJ, Pomper MG and Gorin MA. PSMA-RADS version 1.0: a step towards standardizing the interpretation and reporting of PSMA-targeted PET imaging studies. Eur Urol 2018; 73: 485-487.

[165] Muehlematter UJ, Rupp NJ, Mueller J, Eberli D and Burger IA. 68Ga-PSMA PET/MR-positive, histopathology-proven prostate cancer in a patient with negative multiparametric prostate MRI. Clin Nucl Med 2018; 43: e282-e284.

[166] Simopoulos DN, Natarajan S, Jones TA, Fendler WP, Sisk AE Jr and Marks LS. Targeted prostate biopsy using (68)gallium PSMA-PET/CT for image guidance. Urol Case Rep 2017; 14: 11-14.

[167] Westenfelder KM, Lentes B, Rackerseder J, Navab N, Gschwend JE, Eiber M and Maurer T. Gallium-68 HBED-CC-PSMA positron emission tomography/magnetic resonance imaging for prostate fusion biopsy. Clin Genitourin Cancer 2018; 16: 245-247.

[168] Maurer T, Weirich G, Schottelius M, Weineisen M, Frisch B, Okur A, Kubler H, Thalgott M, Navab N, Schwaiger M, Wester HJ, Gschwend JE and Eiber M. Prostate-specific membrane antigen-radioguided surgery for metastatic lymph nodes in prostate cancer. Eur Urol 2015; 68: 530-534.

[169] Monninkhof EM, van Loon JWL, van Vulpen M, Kerkmeijer LGW, Pos FJ, Haustermans K, van den Bergh L, Isebaert S, McColl GM, Smeenk RJ, Noteboom J, Walraven I, Peeters PHM and van der Heide UA. Standard whole prostate gland radiotherapy with and without lesion boost in prostate cancer: toxicity in the FLAME randomized controlled trial. Radiother Oncol 2018; 127: 74-80.

[170] Zamboglou C, Thomann B, Koubar K, Bronsert P, Krauss T, Rischke HC, Sachpazidis I, Drendel V, Salman N, Reichel K, Jilg CA, Werner M, Meyer PT, Bock M, Baltas D and Grosu AL. Focal dose escalation for prostate cancer using (68)Ga-HBED-CC PSMA PET/CT and MRI: a planning study based on histology reference. Radiat Oncol 2018; 13: 81.

[171] Zamboglou C, Sachpazidis I, Koubar K, Drendel V, Wiehle R, Kirste S, Mix M, Schiller F, Mavroidis P, Meyer PT, Werner M, Grosu AL and Baltas D. Evaluation of intensity modulated radiation therapy dose painting for localized prostate cancer using (68)Ga-HBED-CC PSMA-PET/CT: a planning study based on histopathology reference. Radiother Oncol 2017; 123: 472-477.

[172] Bettermann AS, Zamboglou C, Kiefer S, Jilg CA, Spohn S, Kranz-Rudolph J, Fassbender TF, Bronsert P, Nicolay NH, Gratzke C, Bock M, Ruf J, Benndorf M and Grosu AL. [(68)Ga-]PSMA-11 PET/CT and multiparametric MRI for gross tumor volume delineation in a slice by slice

analysis with whole mount histopathology as a reference standard - Implications for focal radiotherapy planning in primary prostate cancer. Radiother Oncol 2019; 141: 214-219.
[173] Ingrosso G, Becherini C, Lancia A, Caini S, Ost P, Francolini G, Hoyer M, Bottero M, Bossi A, Zilli T, Scartoni D, Livi L, Santoni R, Giacomelli I and Detti B. Nonsurgical salvage local therapies for radiorecurrent prostate cancer: a systematic review and meta-analysis. Eur Urol Oncol 2020; 3: 183-197.
[174] Bouchelouche K and Vendelbo MH. Pulmonary opacities and bronchiectasis avid on 68Ga-PSMA PET. Clin Nucl Med 2017; 42: e216-e217.
[175] Elri T, Aras M, Salihoglu YS, Erdemir RU and Cabuk M. A potential pitfall in the use of (68)Ga-PSMA PET/ct: anthracosis. Rev Esp Med Nucl Imagen Mol 2017; 36: 65-66.
[176] Chan M, Schembri GP and Hsiao E. Serous Cystadenoma of the pancreas showing uptake on 68Ga PSMA PET/CT. Clin Nucl Med 2017; 42: 56-57.
[177] Derlin T, Kreipe HH, Schumacher U and Soudah B. PSMA expression in tumor neovasculature endothelial cells of follicular thyroid adenoma as identified by molecular imaging using 68Ga-PSMA ligand PET/CT. Clin Nucl Med 2017; 42: e173-e174.
[178] Kanthan GL, Drummond J, Schembri GP, Izard MA and Hsiao E. Follicular thyroid adenoma showing avid uptake on 68Ga PSMA-HBED-CC PET/CT. Clin Nucl Med 2016; 41: 331-332.
[179] Law WP, Fiumara F, Fong W and Miles KA. Gallium-68 PSMA uptake in adrenal adenoma. J Med Imaging Radiat Oncol 2016; 60: 514-517.
[180] Malik D, Basher RK, Sood A, Devana SK, Bhattacharya A and Mittal BR. Herniated thoracic spleen mimicking lung metastasis on 68Ga-labeled prostate-specific membrane antigen PET/CT in a patient with prostate cancer. Clin Nucl Med 2017; 42: 485-486.
[181] Stephens M, Kim DI, Shepherd B, Gustafson S and Thomas P. Intense uptake in amyloidosis of the seminal vesicles on 68Ga-PSMA PET mimicking locally advanced prostate cancer. Clin Nucl Med 2017; 42: 147-148.
[182] Kanthan GL, Coyle L, Kneebone A, Schembri GP and Hsiao E. Follicular lymphoma showing avid uptake on 68Ga PSMA-HBED-CC PET/CT. Clin Nucl Med 2016; 41: 500-501.
[183] Vamadevan S, Le K, Bui C and Mansberg R. Prostate-specific membrane antigen uptake in small cleaved B-cell follicular non-hodgkin lymphoma. Clin Nucl Med 2016; 41: 980-981.
[184] Sager S, Vatankulu B, Uslu L and Sonmezoglu K. Incidental detection of follicular thyroid carcinoma in 68Ga-PSMA PET/CT imaging. J Nucl Med Technol 2016; 44: 199-200.
[185] Jena A, Zaidi S, Kashyap V, Jha A and Taneja S. PSMA expression in multinodular thyroid neoplasm on simultaneous Ga-68-PSMA PET/MRI. Indian J Nucl Med 2017; 32: 159-161.
[186] Rauscher I, Maurer T, Steiger K, Schwaiger M and Eiber M. Image of the month: multifocal 68Ga prostate-specific membrane antigen ligand uptake in the skeleton in a man with both prostate cancer and multiple myeloma. Clin Nucl Med 2017; 42: 547-548.
[187] Noto B, Weckesser M, Buerke B, Pixberg M and Avramovic N. Gastrointestinal stromal tumor showing intense tracer uptake on PSMA PET/CT. Clin Nucl Med 2017; 42: 200-202.
[188] Vamadevan S, Shetty D, Le K, Bui C, Mansberg R and Loh H. Prostate-specific membrane antigen (PSMA) avid pancreatic neuroendocrine tumor. Clin Nucl Med 2016; 41: 804-806.
[189] Sasikumar A, Joy A, Nanabala R, Pillai MR, Thomas B and Vikraman KR. (68)Ga-PSMA PET/CT imaging in primary hepatocellular carcinoma. Eur J Nucl Med Mol Imaging 2016; 43: 795-796.
[190] Soydal CAA OE, Demirkazik A and Kucuk NO. Ga-68 PSMA accumulation in hepatocellular carcinoma. Clin Oncol 2016; 1.
[191] Huang YT, Fong W and Thomas P. Rectal carcinoma on 68Ga-PSMA PET/CT. Clin Nucl Med 2016; 41: e167-168.
[192] Stoykow C, Huber-Schumacher S, Almanasreh N, Jilg C and Ruf J. Strong PSMA radioligand uptake by rectal carcinoma: who put the “S” in PSMA? Clin Nucl Med 2017; 42: 225-226.
[193] Lawhn-Heath C, Flavell RR, Glastonbury C, Hope TA and Behr SC. Incidental detection of head and neck squamous cell carcinoma on 68Ga-PSMA-11 PET/CT. Clin Nucl Med 2017; 42: e218-e220.
[194] Shetty D, Loh H, Bui C, Mansberg R and Stevanovic A. Elevated 68Ga prostate-specific membrane antigen activity in metastatic non-small cell lung cancer. Clin Nucl Med 2016; 41: 414-416.
[195] Froehner M, Kuithan F, Zophel K, Heberling U, Laniado M and Wirth MP. Prostate-specific membrane antigen-targeted ligand positron emission tomography/computed tomography and immunohistochemical findings in a patient with synchronous metastatic penile and prostate cancer. Urology 2017; 101: e5-e6.
[196] Hangaard L, Jochumsen MR, Vendelbo MH and Bouchelouche K. Metastases from colorectal cancer avid on 68Ga-PSMA PET/CT. Clin Nucl Med 2017; 42: 532-533.
[197] Gupta M, Choudhury PS, Gupta G and Gandhi J. Metastasis in urothelial carcinoma mimicking prostate cancer metastasis in Ga-68 prostate-specific membrane antigen positron emis-

sion tomography-computed tomography in a case of synchronous malignancy. Indian J Nucl Med 2016; 31: 222-224.

[198] Einspieler I, Tauber R, Maurer T, Schwaiger M and Eiber M. 68Ga Prostate-specific membrane antigen uptake in renal cell cancer lymph node metastases. Clin Nucl Med 2016; 41: e261-262.

[199] Zacho HD, Nielsen JB, Dettmann K, Haberkorn U and Petersen LJ. Incidental detection of thyroid metastases from renal cell carcinoma using 68Ga-PSMA PET/CT to assess prostate cancer recurrence. Clin Nucl Med 2017; 42: 221-222.